

SYNTHESIS AND CATALYTIC ACTIVITY OF LAYERED DOUBLE HYDROXIDE AND METAL
SULFIDE NANOPARTICLE COMPOSITES



A Thesis Submitted in Partial Fulfillment of the Requirements
for the Degree of Master of Science in Chemistry

Department of Chemistry

FACULTY OF SCIENCE

Chulalongkorn University

Academic Year 2021

Copyright of Chulalongkorn University

การสังเคราะห์และกัมมันตภาพในการเร่งปฏิกิริยาของคอมพอสิตของเลเยอร์ดับเบิลไฮดรอกไซด์และ
อนุภาคระดับนาโนเมตรของโลหะซัลไฟด์



วิทยานิพนธ์นี้เป็นส่วนหนึ่งของการศึกษาตามหลักสูตรปริญญาวิทยาศาสตรมหาบัณฑิต
สาขาวิชาเคมี ภาควิชาเคมี
คณะวิทยาศาสตร์ จุฬาลงกรณ์มหาวิทยาลัย
ปีการศึกษา 2564
ลิขสิทธิ์ของจุฬาลงกรณ์มหาวิทยาลัย

อจิวรตี สุวรรณจันทร์ : การสังเคราะห์และกัมมันตภาพในการเร่งปฏิกิริยาของคอมพอสิตของเลเยอร์ดับเบิลไฮดรอกไซด์และอนุภาคระดับนาโนเมตรของโลหะซัลไฟด์. (SYNTHESIS AND CATALYTIC ACTIVITY OF LAYERED DOUBLE HYDROXIDE AND METAL SULFIDE NANOPARTICLE COMPOSITES) อ.ที่ปรึกษาหลัก : ผศ. ดร. นำพล อินสิน

การย่อยสลายสีย้อมเมทิลีนบลูได้นำมาตรวจสอบกระบวนการเร่งปฏิกิริยาโดยใช้คอมพอสิตของเลเยอร์ดับเบิลไฮดรอกไซด์และอนุภาคระดับนาโนเมตรของโลหะซัลไฟด์ คอมพอสิตของเลเยอร์ดับเบิลไฮดรอกไซด์และอนุภาคระดับนาโนเมตรของโลหะซัลไฟด์ถูกสังเคราะห์โดยวิธีไฮโดรเทอร์มอล และคอมโพสิตถูกพิสูจน์เอกลักษณ์ด้วยเทคนิควิเคราะห์การเลี้ยวเบนของรังสีเอกซ์และวิเคราะห์ด้วยกล้องจุลทรรศน์อิเล็กตรอนแบบส่องกราด โลหะซัลไฟด์ และ เลเยอร์ดับเบิลไฮดรอกไซด์ มีขนาด 350-450 นาโนเมตร และ 2200-3500 นาโนเมตรตามลำดับ คอมโพสิตถูกบรรจุด้วย 1.8, 3.4, 5.2 และ 9.9 ร้อยละโดยน้ำหนักของโลหะซัลไฟด์ โลหะซัลไฟด์, เลเยอร์ดับเบิลไฮดรอกไซด์ และ คอมพอสิตของเลเยอร์ดับเบิลไฮดรอกไซด์และอนุภาคระดับนาโนเมตรของโลหะซัลไฟด์ ถูกทดสอบด้วยภายใต้สภาวะเดียวกันในการย่อยสลายสีย้อมเมทิลีนบลู คอมพอสิตของเลเยอร์ดับเบิลไฮดรอกไซด์และอนุภาคระดับนาโนเมตรของโลหะซัลไฟด์ที่มีโลหะซัลไฟด์ตัวอย่างที่ 18 ให้ผลการสลายสีย้อมที่สูงกว่าเมื่อเปรียบเทียบกับทั้งของเลเยอร์ดับเบิลไฮดรอกไซด์ และโลหะซัลไฟด์ผ่านปฏิกิริยาเฟนต์เหมือน อิทธิพลของค่าความเป็นกรด, ความเข้มข้นของสีย้อม, ปริมาณของตัวเร่งปฏิกิริยาและปริมาณของไฮโดรเจนเปอร์ออกไซด์ได้ถูกศึกษาด้วย โดยที่สภาวะเหมาะสมของคอมพอสิตของเลเยอร์ดับเบิลไฮดรอกไซด์และอนุภาคระดับนาโนเมตรของโลหะซัลไฟด์ที่มีโลหะซัลไฟด์ตัวอย่างที่ 18 สามารถสลายสีย้อมเมทิลีนบลูได้ 97.9 เปอร์เซ็นต์ ภายในเวลา 240 นาที กลไกในการเกิดปฏิกิริยาได้ถูกตรวจสอบ คอมพอสิตของเลเยอร์ดับเบิลไฮดรอกไซด์และอนุภาคระดับนาโนเมตรของโลหะซัลไฟด์ ที่เตรียมได้ในงานวิจัยนี้ถูกพิสูจน์ว่าเป็นตัวเร่งปฏิกิริยาที่มีประสิทธิภาพสำหรับการใช้บำบัดน้ำเสีย

สาขาวิชา เคมี
ปีการศึกษา 2564

ลายมือชื่อนิสิต
ลายมือชื่อ อ.ที่ปรึกษาหลัก

6172149523 : MAJOR CHEMISTRY

KEYWORD: degradation; layered double hydroxide; metal sulfide; Fenton

Ajirawadee Suwanchan : SYNTHESIS AND CATALYTIC ACTIVITY OF LAYERED
DOUBLE HYDROXIDE AND METAL SULFIDE NANOPARTICLE COMPOSITES.

Advisor: Asst. Prof. Dr. Numpon Insin

Degradation of methylene blue dye was investigated over heterogenous catalytic process using layered double hydroxide and metal sulfide nanoparticle composites. $\text{CuCo}_2\text{S}_4/\text{NiFe}$ LDH nanocomposites were synthesized using hydrothermal method, and the composites were characterized by SEM and XRD techniques. CuCo_2S_4 and NiFe LDH were formed with an average particle in the range of 350-450 nm and 2200-3500 nm, respectively. The composites were loaded at 1.8, 3.4, 5.2 and 9.9 wt% of CuCo_2S_4 . CuCo_2S_4 , NiFe LDH and $\text{CuCo}_2\text{S}_4/\text{NiFe}$ LDH composites were tested at the same condition for methylene blue degradation. The 18 $\text{CuCo}_2\text{S}_4/\text{NiFe}$ LDH composites provided higher catalytic degradation of methylene blue compared to both CuCo_2S_4 and NiFe LDH through Fenton-like reaction. Effect of pH, dye concentration, amount of catalyst and amount of H_2O_2 were studied. At the optimized condition of 18 $\text{CuCo}_2\text{S}_4/\text{NiFe}$ LDH nanocomposites, percent degradation of methylene reached 97.9 within 240 min. Proposed mechanisms were investigated. $\text{CuCo}_2\text{S}_4/\text{NiFe}$ LDH nanocomposites prepared in this work were proved to be efficient catalysts for wastewater treatment application.

Field of Study: Chemistry

Student's Signature

Academic Year: 2021

Advisor's Signature

ACKNOWLEDGEMENTS

The completion of this research could not have been possible without the expertise of following individuals. Firstly, I would like to express my deep appreciation and indebtedness to my beloved advisor, Assistant Dr. Numpon Insin, for giving me the opportunity to be part of NI Laboratory members. It has been a great opportunity to work with him through these past years.

Special gratitude is also owed to Professor Dr. Vudhichai Parasuk, who has been the chairman, Assistant Professor Dr. Pannee Leeladee and Assoc Professor Dr. Tosapol Maluangnont as examiner of this thesis committee for useful suggestion and invaluable discussion throughout this research.

Finally, thank to my supportive NI Laboratory members; without you none of this would indeed be possible.

Ajirawadee Suwanchan

TABLE OF CONTENTS

	Page
.....	iii
ABSTRACT (THAI).....	iii
.....	iv
ABSTRACT (ENGLISH).....	iv
ACKNOWLEDGEMENTS.....	v
TABLE OF CONTENTS.....	vi
LIST OF TABLES.....	ix
LIST OF FIGURES.....	x
CHAPTER I INTRODUCTION.....	1
1.1 Rational.....	1
1.2 Objectives.....	2
1.3 Expected beneficial outcome.....	2
CHAPTER II THEORY AND LITERATURE REVIEWS.....	3
2.1 Methylene blue.....	3
2.1.1 Properties.....	3
2.1.2 Toxicity.....	4
2.2 Advanced oxidation process.....	5
2.3 Fenton process.....	6
2.4 Fenton like reaction.....	6
2.5 Layered double hydroxides.....	6
2.6 Metal sulfide.....	9

CHAPTER III METHODOLOGY.....	12
3.1 Catalyst preparation.....	12
3.1.1 Materials.....	12
3.1.2 Synthesis of CuCo_2S_4	13
3.1.3 Synthesis of $\text{CuCo}_2\text{S}_4/\text{NiFe}$ LDH.....	13
3.2 Catalyst characterization.....	13
3.2.1 X-ray diffraction (XRD).....	13
3.2.2 Scanning electron microscope (SEM).....	14
3.2.3 Inductively coupled plasma optical emission spectroscopy (ICP-OES).....	14
3.3 The reaction study in catalytic degradation of methylene blue.....	14
3.3.1 Catalytic degradation of methylene blue procedure.....	14
CHAPTER IV RESULTS AND DISCUSSION.....	15
4.1 X-ray diffraction (XRD).....	15
4.2 Scanning electron microscope (SEM).....	16
4.3 Energy dispersive X-ray spectroscopy (EDS).....	18
4.3 Inductively coupled plasma optical emission spectroscopy (ICP-OES).....	28
4.4 Catalytic performance.....	29
4.4.1 Effect of H_2O_2	31
4.4.2 Effect of catalyst dosage.....	32
4.4.3 Effect of dye concentration.....	33
4.4.4 Effect of pH.....	34
4.5 Catalytic mechanism.....	36
CHAPTER V CONCLUSION.....	39
5.1 Conclusion.....	39

5.2 Recommendations for future work.....	39
REFERENCES	40
VITA.....	43



LIST OF TABLES

	Page
Table 1 Physical properties of methylene blue dye [9]	4
Table 2 Materials for CuCo_2S_4 synthesis	12
Table 3 Materials for NiFe LDH synthesis	12
Table 4 Organic dye compound.....	12
Table 5 Materials for pH adjustment.....	12
Table 6 Elemental percentages of NiFe LDH	19
Table 7 Elemental percentages of CuCo_2S_4	20
Table 8 Elemental percentages of $18\text{CuCo}_2\text{S}_4/\text{NiFe}$ LDH	22
Table 9 Elemental percentages of $34\text{CuCo}_2\text{S}_4/\text{NiFe}$ LDH	24
Table 10 Elemental percentages of $52\text{CuCo}_2\text{S}_4/\text{NiFe}$ LDH	26
Table 11 Elemental percentages of $99\text{CuCo}_2\text{S}_4/\text{NiFe}$ LDH	28
Table 12 The molar ratios of Ni:Fe of initials and final value	28
Table 13 The molar ratios of Cu:Co of initials value and final value.....	29
Table 14 Metal leaching in the reaction mixture at different pH after Fenton reaction	35

LIST OF FIGURES

	Page
Figure 1 The model and the structure of methylene blue [8]	3
Figure 2 Harmful effects of MB dye [10].....	5
Figure 3 Schematic diagram explaining the processes involved in AOPS [11].....	5
Figure 4 Schematic representation of the classical LDHs structure [13].....	7
Figure 5 Methylene blue removal percentages obtained in the LDH through Fenton-like reaction.	7
Figure 6 Degradation of methyl orange on different catalysts.....	8
Figure 7 The degradation of MO on CuAl-LDH/ MgO ₂ -50	8
Figure 8 Effect of various scavengers on NiFe LDH for MB degradation.....	9
Figure 9 UV-vis spectra on CuS during the degradation of MB.....	10
Figure 10 UV-vis spectra on CuS during the degradation of the mixed solution of MB and Rh B	10
Figure 11 Degradation of MB on CuS, CoS, CuCo ₂ S ₄ and CuCo ₂ S ₄ /MWCNTs.....	11
Figure 12 XRD patterns of CuCo ₂ S ₄ , NiFe LDH and CuCo ₂ S ₄ /NiFe LDH composites....	15
Figure 13 SEM images of a) NiFe LDH, b) CuCo ₂ S ₄ , c) 18CuCo ₂ S ₄ /NiFe LDH,.....	18
Figure 14 EDS elemental mapping images of NiFe LDH.....	19
Figure 15 EDS elemental mapping images of CuCo ₂ S ₄	20
Figure 16 EDS elemental mapping images of 18CuCo ₂ S ₄ /NiFe LDH.....	21
Figure 17 EDS elemental mapping images of 34CuCo ₂ S ₄ /NiFe LDH.....	23
Figure 18 EDS elemental images of 52CuCo ₂ S ₄ /NiFe LDH.....	25
Figure 19 EDS elemental images of 99CuCo ₂ S ₄ /NiFe LDH.....	27
Figure 20 Degradation of methylene blue on CuCo ₂ S ₄ /NiFe LDH	30

Figure 21 Effect of H ₂ O ₂ volume on dye degradation.....	31
Figure 22 Effect of catalyst dosage on dye degradation.....	32
Figure 23 Effect of methylene blue concentration on dye degradation	33
Figure 24 Effect of pH on dye degradation.....	34
Figure 25 Effect of various scavengers on dye degradation.....	36
Figure 26 Scheme illustrating the mechanism of the enhance catalytic process of CuCo ₂ S ₄ /NiFeLDH	38



CHAPTER I INTRODUCTION

1.1 Rational

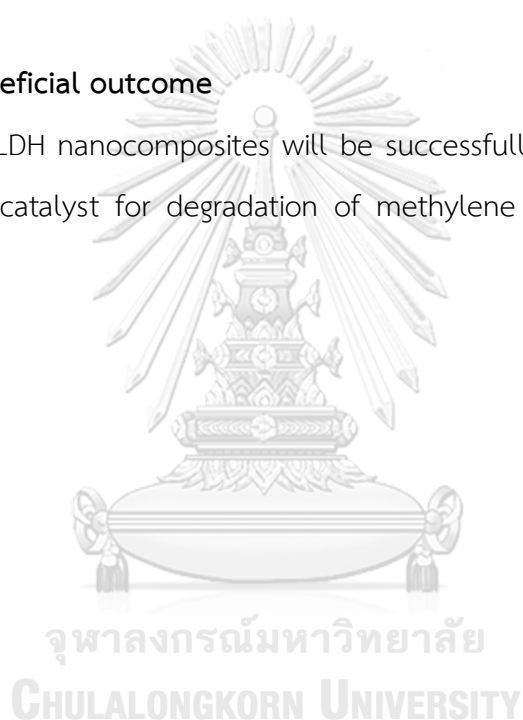
Advanced oxidation processes (AOPs) have been widely used for treating various industrial wastewaters contaminated by organic compounds using hydroxy radical (OH^*) and other reactive oxygen species (ROS). Fenton reaction is one of the most common method for rapid degradation of organic contaminants.[1],[2] Layered double hydroxides (LDH) are two-dimensional clay materials consisted of divalent and trivalent cations located in edge-sharing octahedral structure and anion in the interlayer space. LDH have applications in various fields including adsorbents, catalysis, photocatalysis, photochemistry, electrochemistry, biomedical science, magnetization, polymerization and environmental applications.[3] LDH have been considered as a catalyst on Fenton process due to the highly dispersed metals, flexibility in composition, chemical stability, unique structural and reusability of materials.[4] NiFe LDH was gained attention owing to nontoxic nature, resource abundance and environmental-friendliness for verification of catalytic degradation materials.[5] Metal sulfide has been demonstrated to be excellent co-catalysts to enhance efficiency of H_2O_2 decomposition to generate reactive species. CuCo_2S_4 has provided multiple redox stage leading to benefit reaction process.[6] LDH containing heterostructure have attracted attention because the composites can keep characteristic of each component, enhance catalytic activity and increase the whole properties of the composites.[7] In this work, $\text{CuCo}_2\text{S}_4/\text{NiFe}$ LDH composites were fabricated by hydrothermal method. Degradation of methylene blue was performed through a Fenton-like reaction.

1.2 Objectives

1. To synthesize and characterize $\text{CuCo}_2\text{S}_4/\text{NiFe}$ LDH nanocomposites with various wt% loading of CuCo_2S_4
2. To investigate the effect of H_2O_2 volume, catalyst dosage, methylene blue concentration and pH on dye degradation of Fenton-like process.
3. To propose mechanism of $\text{CuCo}_2\text{S}_4/\text{NiFe}$ LDH nanocomposites related to Fenton-like reaction.

1.3 Expected beneficial outcome

$\text{CuCo}_2\text{S}_4/\text{NiFe}$ LDH nanocomposites will be successfully synthesized and can be used as efficient catalyst for degradation of methylene blue through Fenton-like reaction.



CHAPTER II THEORY AND LITERATURE REVIEWS

2.1 Methylene blue

2.1.1 Properties

Methylene blue is an organic chloride salt with a formula $C_{16}H_{18}ClN_3S$. Methylene blue has many synonyms such as methylthioninium chloride or Swiss blue. Methylene blue is used as a potential dye in many applications such as textile, pharmaceutical, paper, dyeing, printing, paint, medicine, and food industries. The physical properties are shown in Table 1



Figure 1 The model and the structure of methylene blue [8]

Table 1 Physical properties of methylene blue dye [9]

Property	Value
Color Index (C.I.)	52030
Trade name	Methylene Blue
Scientific name	Basic Blue 9
Color	Dark green to blue crystals or powder
Maximum wavelength (λ_{\max}) (nm)	665
Molecular diffusivity (D_{mol}) (at 25°C)	4.7×10^{-6} (cm ² /s)
Solubility in water	Soluble in water
Chemical formula	$\text{C}_{16}\text{H}_{18}\text{N}_3\text{OS} \cdot 3\text{H}_2\text{O}$
Molecular weight	373.5 (g/g mol)
Molecular volume	390.2 (cm ³ /g mol)

2.1.2 Toxicity

Methylene blue dyes from textile industries are important organic pollutant which were released as wastewater to natural water sources leading to harmful effects directly to human being and aquatic life. Due to the toxicity, carcinogenic substance and non-biodegradable materials of the dyes, MB is considered as substantial toxicity. For human health, MB causes nausea, diarrhea, vomiting, dizziness, headache, fever, anemia, irritation of mouth, throat, esophagus and stomach, irritation of skin with redness and itching, discoloration of urine, and bladder irritation as shown in Fig. 2.

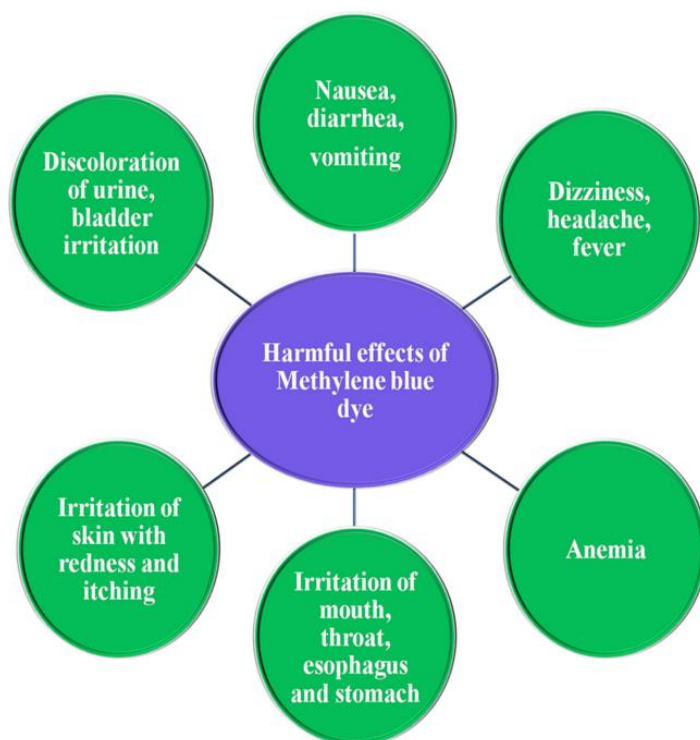


Figure 2 Harmful effects of MB dye [10]

2.2 Advanced oxidation process

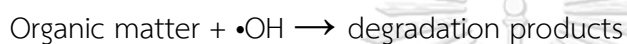
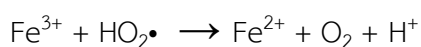
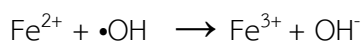
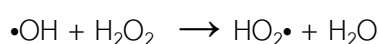
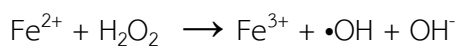
According to the harmful impacts of MB in wastewater from the textile industries, wastewater treatment is considered as an important process for discharging into the ecosystem. Advanced oxidation processes have been studied as a promising method for organic pollutant removal from water. AOPs are oxidation chemical processes generating reactive species such as hydroxy radical ($\bullet\text{OH}$). The production of hydroxy radicals can carry out the destruction of toxic pollutant (in Fig. 3) without generating any additional harmful substances.



Figure 3 Schematic diagram explaining the processes involved in AOPS [11]

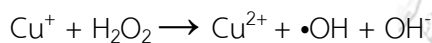
2.3 Fenton process

Fenton reaction is a reaction of iron ions and oxidizing agent to enhance oxidative potential of oxidizing agent. The general mechanism can be presented following equations [12]



2.4 Fenton like reaction

Fenton like reaction is replacing of Fe^{2+} by other metal such as copper and cobalt.



2.5 Layered double hydroxides

Layered double hydroxides (LDH) are synthetic clay with two-dimensional materials structure consisting of metal cation octahedrally coordinated by hydroxide ions connected each other in the layer stacked together with anion in the interlayer space for charge balance. The general formular of LDHs is $[\text{M}^{2+}_{1-x} \text{M}^{3+}_x(\text{OH})_2]^{x+}[\text{A}_{x/n}]^{n-} \cdot m\text{H}_2\text{O}$, where M^{2+} and M^{3+} are metal cations, A is an intercalate anion (CO_3^{2-} , SO_4^{2-} , NO_3^- , F^- or Cl^-) as shown in Fig. 4.

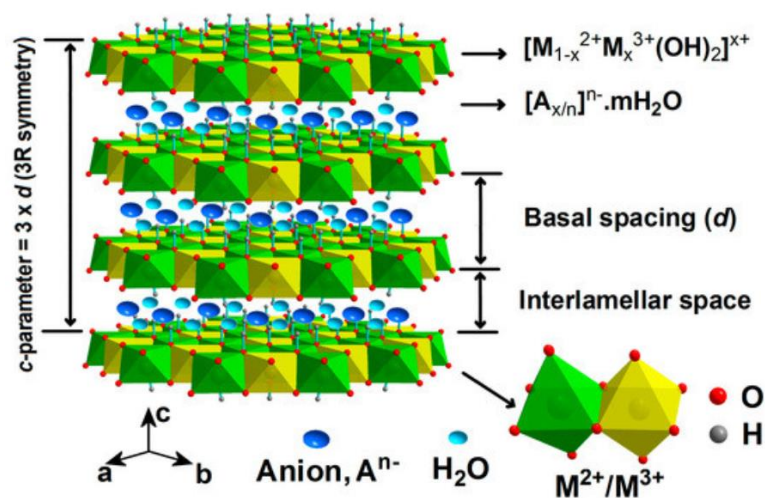


Figure 4 Schematic representation of the classical LDHs structure [13]

LDH have been considered as a Fenton catalyst due to their ion exchange properties and high surface area. R.G.L. Goncaves et al. [4] reported MgFe-LDH and MnMgFe-LDH can be used as an efficient Fenton like catalyst for MB removal for 5 reaction cycles.

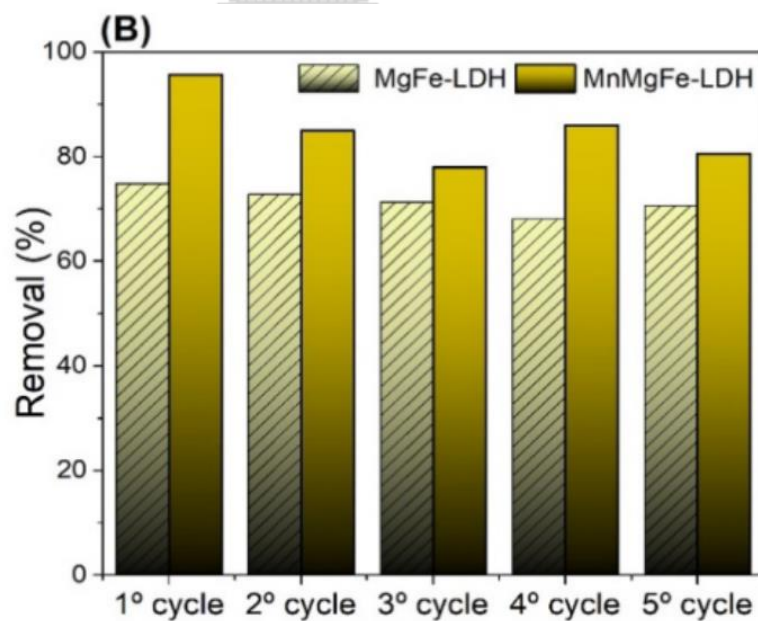


Figure 5 Methylene blue removal percentages obtained in the LDH through Fenton-like reaction.

S. G. Aragaw et al. [14] interested in CuAl-LDH/ MgO₂ composite for degradation of methyl orange through Fenton-like process. CuAl-LDH/ MgO₂ composite with 50:50 ratio of LDH and MgO₂ showed 97% MO degradation.

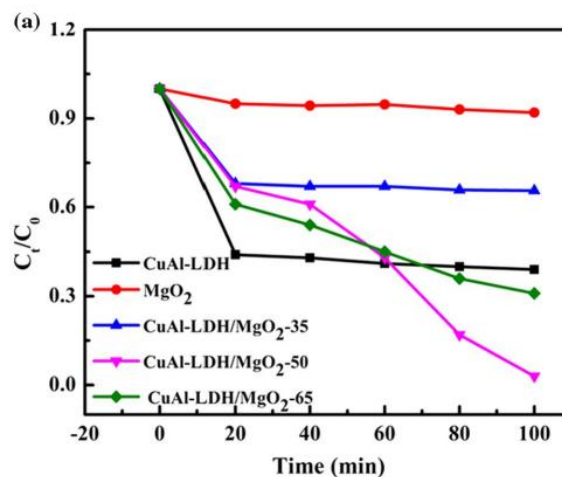


Figure 6 Degradation of methyl orange on different catalysts

They proposed mechanism as shown in Fig. 7. When MO dye is adsorbed on the surface of the catalyst H₂O₂ was generated from MgO₂ in aqueous system. CuAl LDH activated H₂O₂ to reactive species. Once the MO dye reacted with reactive species, Degradation products were formed.

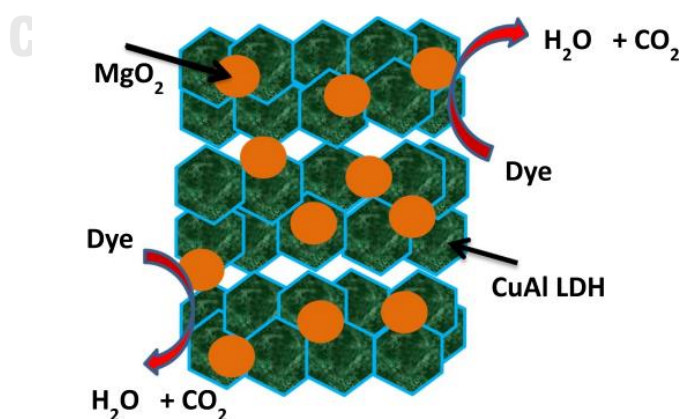


Figure 7 The degradation of MO on CuAl-LDH/ MgO₂-50

Q. Wang et al. [15] prepared NiFe LDH with difference method for MB removal in Fenton-like processes. NiFe LDH both which was prepared using coprecipitation and hydrothermal process showed high performance for degradation of MB. The Addition of NaN_3 and KI into the system showed the decrease of dye removal indicating formation of active radicals.

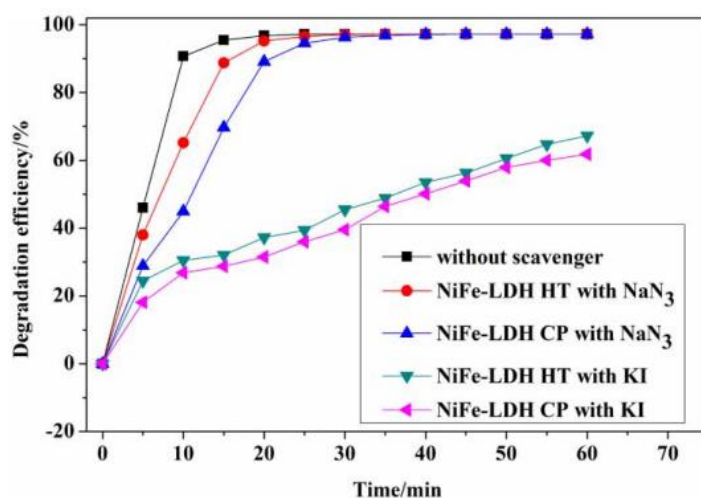


Figure 8 Effect of various scavengers on NiFe LDH for MB degradation

According to previous literature reviews, LDH can be active catalyst for Fenton-like reaction. For this reason, LDH will be promising catalytic Fenton-like processes.

2.6 Metal sulfide

Metal sulfide have attracted attention as excellent H_2O_2 catalytic oxidation. Z. Li et al. [16] investigated dye decolorization of methylene blue and rhodamine B on CuS. The change in UV-vis spectra during the removal of MB and mixture of the mixed solution (MB and Rh B) are shown in Fig. 9 and 10.

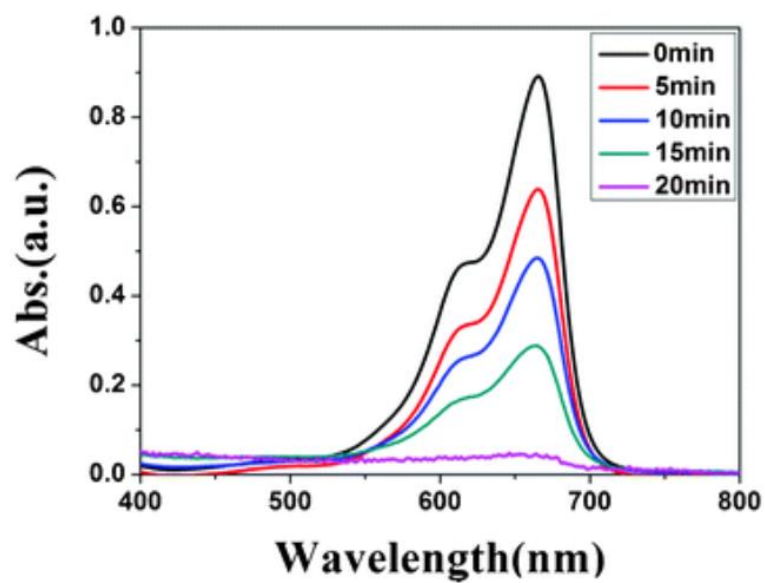


Figure 9 UV-vis spectra on CuS during the degradation of MB

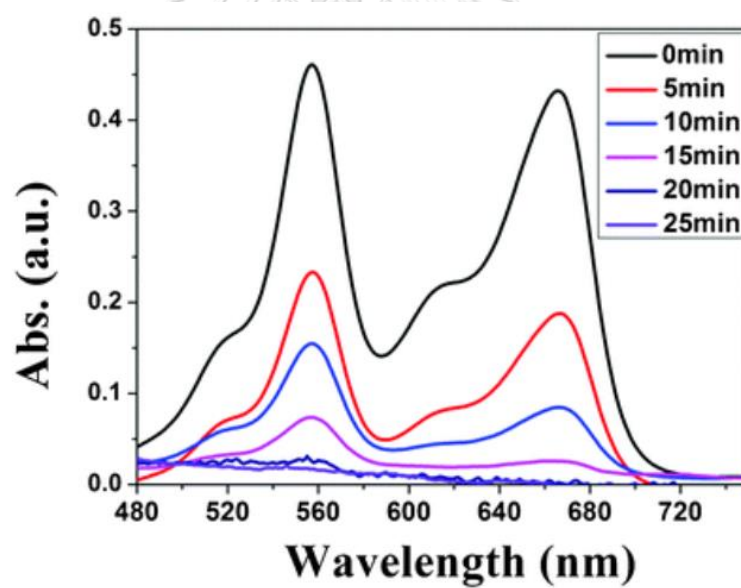


Figure 10 UV-vis spectra on CuS during the degradation of the mixed solution of MB and Rh B

Moreover, fabrication of metal sulfide with good conductivity materials enhanced catalytic performance. M. Zhang et al. synthesized $\text{CuCo}_2\text{S}_4/\text{MWCNTs}$ for catalytic MB degradation. The $\text{CuCo}_2\text{S}_4/\text{MWCNTs}$ catalytic materials provide high performance as shown in Fig. 11.

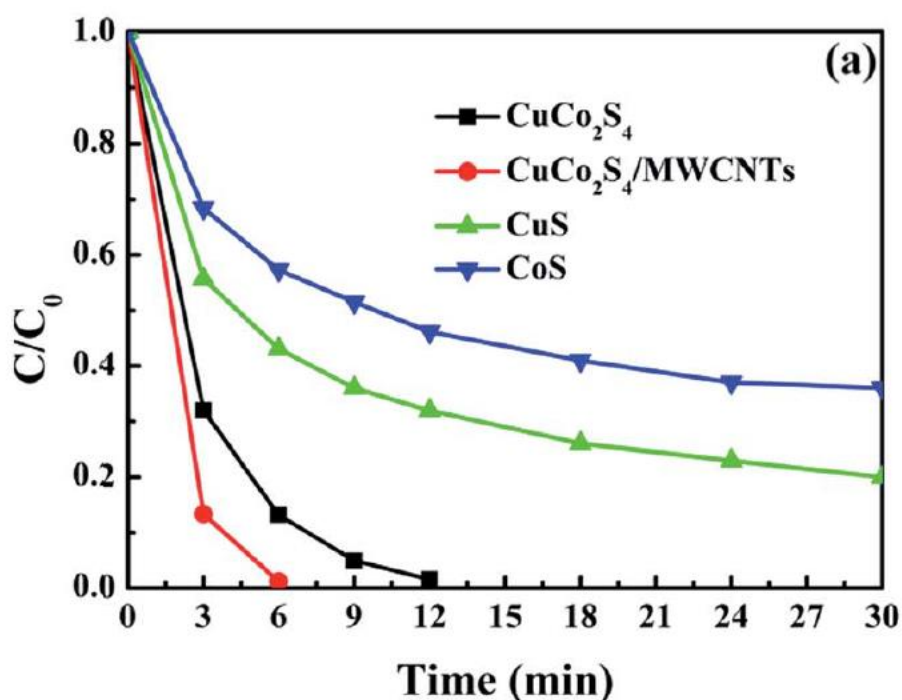


Figure 11 Degradation of MB on CuS , CoS , CuCo_2S_4 and $\text{CuCo}_2\text{S}_4/\text{MWCNTs}$

Due to the efficient catalytic degradation of metal sulfide, It has been considered to be co-catalysts to improve catalytic activity of Fenton-like processes.

According to benefit of LDH and metal sulfide, heterostructure of these two materials are interesting to enhance catalytic performance for H_2O_2 decomposition. This research aimed to preparation of nanocomposites of CuCo_2S_4 and NiFe LDH for catalytic degradation of MB dye.

CHAPTER III METHODOLOGY

3.1 Catalyst preparation

3.1.1 Materials

All chemicals are of analytical grade and used as received without further purification.

Table 2 Materials for CuCo_2S_4 synthesis

Name	Formular	Company
Cobalt(II) nitrate hexahydrate	$\text{Co}(\text{NO}_3)_2 \cdot 6\text{H}_2\text{O}$	Merk
Copper(II) nitrate trihydrate	$\text{Cu}(\text{NO}_3)_2 \cdot 3\text{H}_2\text{O}$	Merk
Thiourea	$\text{CH}_4\text{N}_2\text{S}$	TCI
Ethylenediamine	$\text{C}_2\text{H}_8\text{N}_2$	SRL

Table 3 Materials for NiFe LDH synthesis

Name	Formular	Company
Nickel(II) nitrate hexahydrate	$\text{Ni}(\text{NO}_3)_2 \cdot 6\text{H}_2\text{O}$	Merk
Iron(III) nitrate nonahydrate	$\text{Fe}(\text{NO}_3)_3 \cdot 9\text{H}_2\text{O}$	Merk
Uria	$\text{CH}_4\text{N}_2\text{O}$	Sigma-Aldrich

Table 4 Organic dye compound

Name	Formular	Company
Methylene Blue	$\text{C}_{16}\text{H}_{18}\text{ClN}_3\text{S}$	Sigma-Aldrich

Table 5 Materials for pH adjustment

Name	Formular	Company
Sodium chloride	NaOH	Ajax Finechem
Perchloric acid	HClO_4	Loba Chemie

3.1.2 Synthesis of CuCo_2S_4

CuCo_2S_4 was prepared by using simple hydrothermal method.[17] Firstly, a mixture solution of 1 mmol of $\text{Cu}(\text{NO}_3)_2 \cdot 3\text{H}_2\text{O}$ and 2 mmol of $\text{Co}(\text{NO}_3)_2 \cdot 6\text{H}_2\text{O}$ was dissolved in 40 mL of distilled water. The solution was stirred for 10 min. Then 4 mmol of thiourea was added to the solution of metal precursors followed by vigorous stirring for 15 min. 2 mL of ethylenediamine was added to the clear solution. The whole brown solution was transferred to a 100 mL Teflon-lined autoclave. The autoclave was sealed followed by heating at 200°C for 24 h. After hydrothermal treatment the vessel was cooled down to room temperature naturally. The black-colored product was collected by centrifugation and washing with distilled water and ethanol several times before drying in an oven at 50 °C overnight.

3.1.3 Synthesis of $\text{CuCo}_2\text{S}_4/\text{NiFe}$ LDH

In a typical preparation of $\text{CuCo}_2\text{S}_4/\text{NiFe}$ LDH, an appropriate amount of CuCo_2S_4 was added into 40 mL of distilled water with magnetic stirring for 10 min followed by the addition of 0.9 mmol of $\text{Ni}(\text{NO}_3)_2 \cdot 6\text{H}_2\text{O}$ and 0.3 mmol of $\text{Fe}(\text{NO}_3)_3 \cdot 9\text{H}_2\text{O}$. Then 0.12 mmol of urea was added to the black solution. After stirring for another 15 min, the whole solution was transferred to the 100 mL Teflon-lined autoclave. The autoclave was sealed and kept at 120 °C for 24 h. The reaction mixture was allowed to cool down to room temperature. The final solid product was washed with distilled water and ethanol several times and dried in at 50°C overnight.[18] The $\text{CuCo}_2\text{S}_4/\text{NiFe}$ LDH composites at 1.8, 3.4, 5.2, and 9.9 wt% of CuCo_2S_4 loading were synthesized and named as 18 $\text{CuCo}_2\text{S}_4/\text{NiFe}$ LDH, 34 $\text{CuCo}_2\text{S}_4/\text{NiFe}$ LDH 52 $\text{CuCo}_2\text{S}_4/\text{NiFe}$ LDH and 99 $\text{CuCo}_2\text{S}_4/\text{NiFe}$ LDH, respectively.

3.2 Catalyst characterization

3.2.1 X-ray diffraction (XRD)

The crystallinity and phase identification were investigated using X-ray powder diffractometer (XRD) on a Rigaku SmartLab 30kV with Cu $K\alpha$ radiation, which was set an accelerating voltage of 40 kV and applied current of 30 mA.

3.2.2 Scanning electron microscope (SEM)

The morphology of the catalysts was observed using a scanning electron microscope (SEM) on JEOL JSM-IT100 at 20kV.

3.2.3 Inductively coupled plasma optical emission spectroscopy (ICP-OES)

Metal content and Metal leaching are determined by ICP-OES, Thermo Scientific, iCAP 6500.

3.3 The reaction study in catalytic degradation of methylene blue

3.3.1 Catalytic degradation of methylene blue procedure

10 mg of the catalyst was added into a bottle containing of 50 mL 10 ppm methylene blue. The reaction was stirred in the dark for 1 h to reach adsorption-desorption equilibrium. 200 μL of H_2O_2 was added to the solutions to start the reaction. UV visible spectrophotometer (Agilent HP 8453) was performed to monitor methylene blue degradation. The blue dye solution absorbed at 664 nm. The spectra were recorded in the range 400-800 nm.

CHAPTER IV RESULTS AND DISCUSSION

4.1 X-ray diffraction (XRD)

The XRD patterns of CuCo_2S_4 in Fig.12 showed peaks at 16.13° , 26.59° , 31.27° , 37.97° , 46.99° , 49.99° and 54.73° indicating (111) (022), (113), (004), (224), (115) and (044) planes, respectively, which agrees with the CuCo_2S_4 standard pattern (JCPDS card no.42–1450). The diffraction pattern of NiFe LDH showed peaks at 11.35° , 22.74° and 35.42° corresponding to (003), (006) and (009) planes, respectively, which are characteristic of an LDH phase. The $\text{CuCo}_2\text{S}_4/\text{NiFe}$ LDH showed no impurity peaks confirming successful synthesis of the composites.

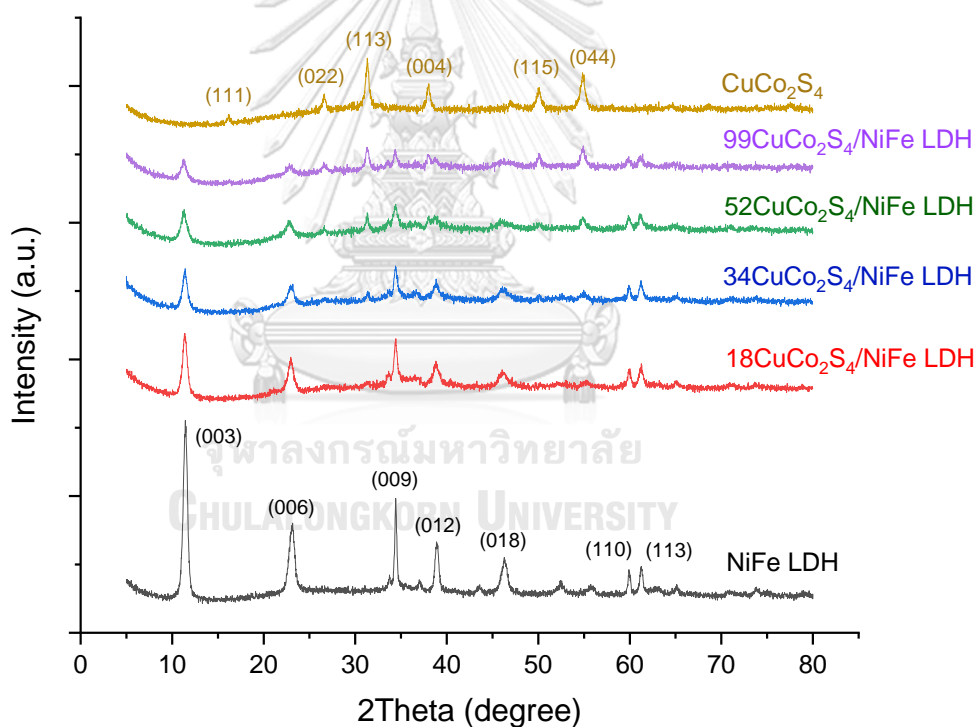
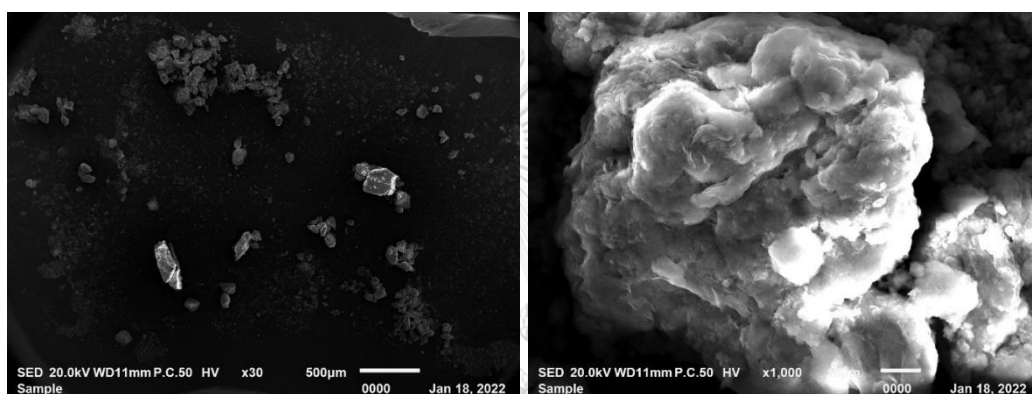


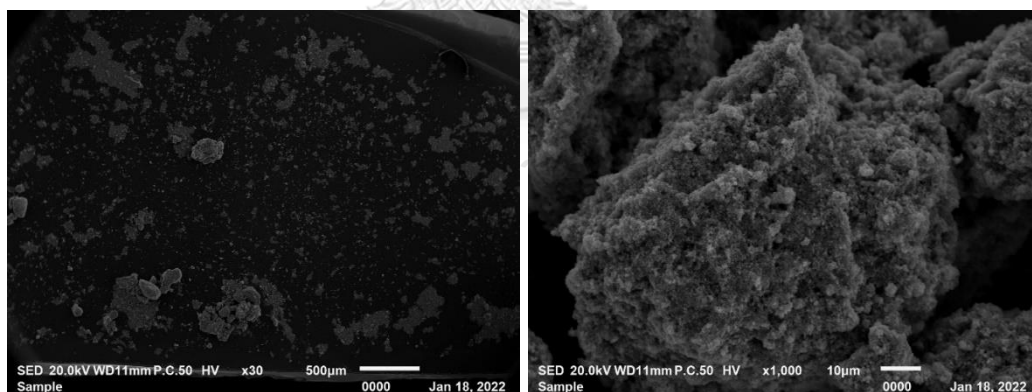
Figure 12 XRD patterns of CuCo_2S_4 , NiFe LDH and $\text{CuCo}_2\text{S}_4/\text{NiFe}$ LDH composites

4.2 Scanning electron microscope (SEM)

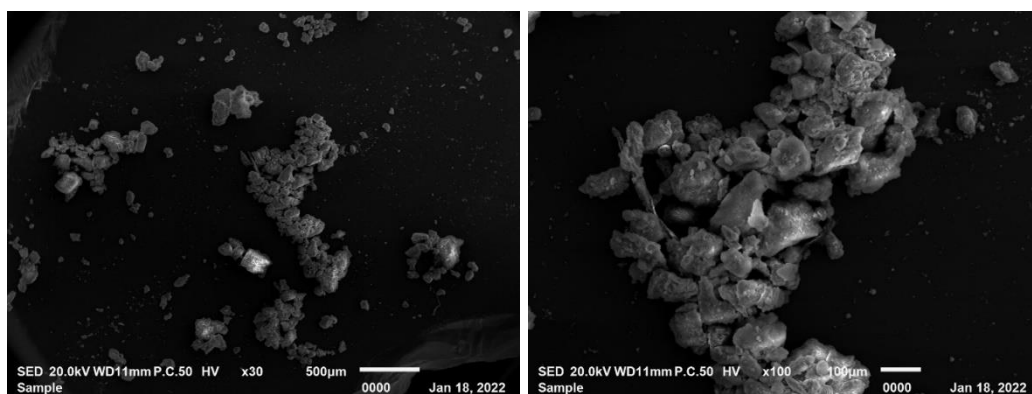
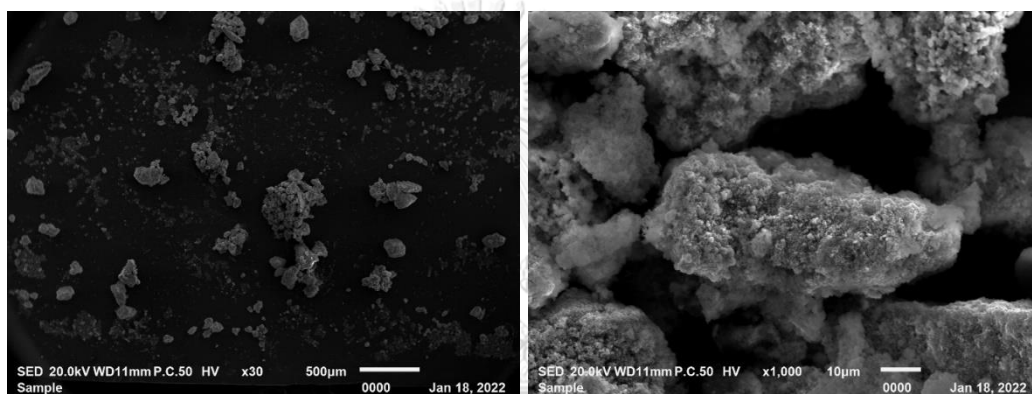
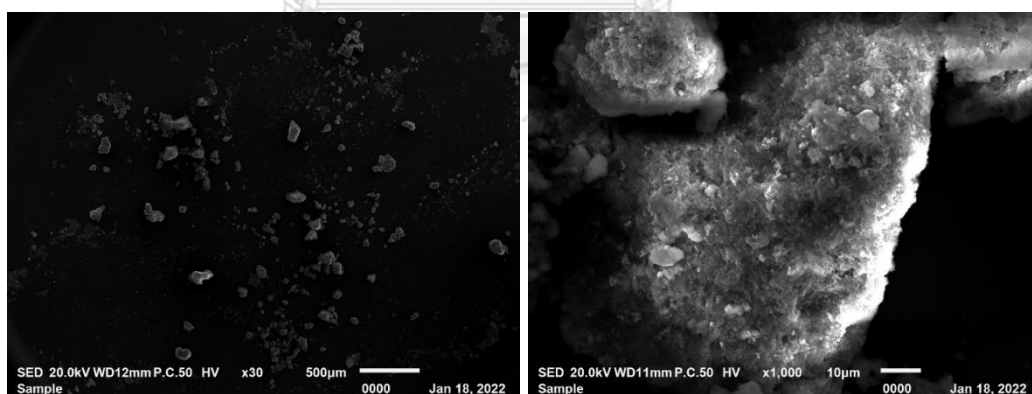
The SEM images of the as-prepared CuCo_2S_4 , NiFe LDH and $18\text{CuCo}_2\text{S}_4/\text{NiFe}$ LDH composites are shown in Fig. 13 a)-f). CuCo_2S_4 presented rough surface with the sizes of 350-450 nm, whereas NiFe LDH showed more smooth surface with average sizes in range of 2200-3500 nm. After loading of CuCo_2S_4 to NiFe LDH, the surface of composites became rougher indicating deposition of CuCo_2S_4 on the surface of NiFe LDH.



a) NiFe LDH



b) CuCo_2S_4

c) 18CuCo₂S₄/NiFe LDHd) 34CuCo₂S₄/NiFe LDHe) 52CuCo₂S₄/NiFe LDH

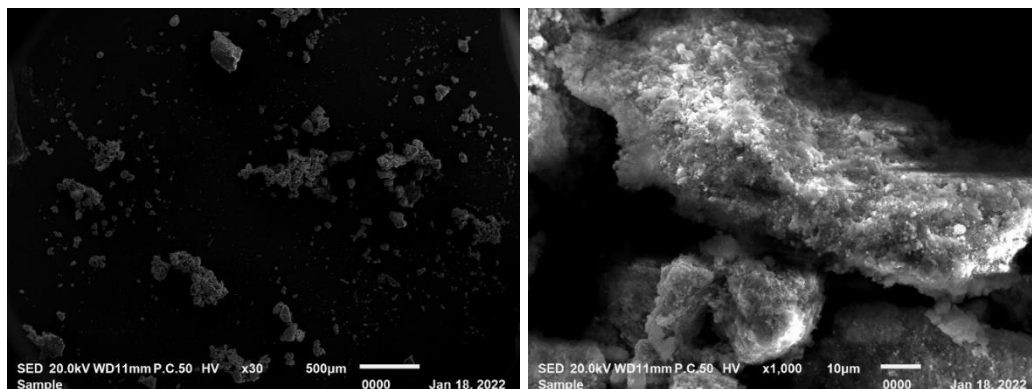
f) $99\text{CuCo}_2\text{S}_4/\text{NiFe}$ LDH

Figure 13 SEM images of a) NiFe LDH, b) CuCo_2S_4 , c) $18\text{CuCo}_2\text{S}_4/\text{NiFe}$ LDH, d) $34\text{CuCo}_2\text{S}_4/\text{NiFe}$ LDH, e) $52\text{CuCo}_2\text{S}_4/\text{NiFe}$ LDH and f) $99\text{CuCo}_2\text{S}_4/\text{NiFe}$ LDH

4.3 Energy dispersive X-ray spectroscopy (EDS)

EDS elemental mapping images showed the clear dispersion and uniformly distribution of Ni, Fe, O and C for NiFe LDH and $\text{CuCo}_2\text{S}_4/\text{NiFe}$ LDH composites. The presence of Cu, Co and S was confirmed in CuCo_2S_4 and $\text{CuCo}_2\text{S}_4/\text{NiFe}$ LDH composites. Due to the less loading of CuCo_2S_4 in $18\text{CuCo}_2\text{S}_4/\text{NiFe}$ LDH, no Cu and Co presented in EDS result. In addition, the elemental percentages were shown in Table 6-11.

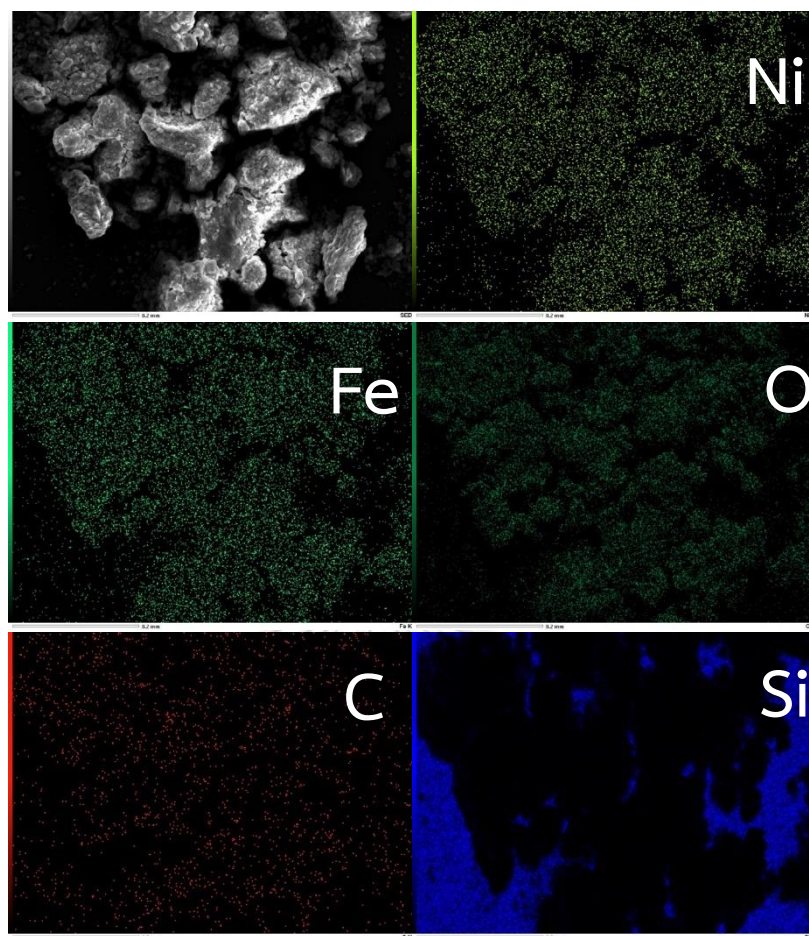


Figure 14 EDS elemental mapping images of NiFe LDH

Table 6 Elemental percentages of NiFe LDH

Formula	mass%	Atom%	Sigma	Net	K ratio	Line
C	8.58	17.6	0.06	2199	0.000703	K
O	5	7.71	0.05	10017	0.010869	K
Si	83.93	73.63	0.12	1554558	0.60598	K
Fe	0.93	0.41	0.03	4423	0.006146	K
Ni	1.56	0.66	0.04	5449	0.010648	K
Total	100	100				

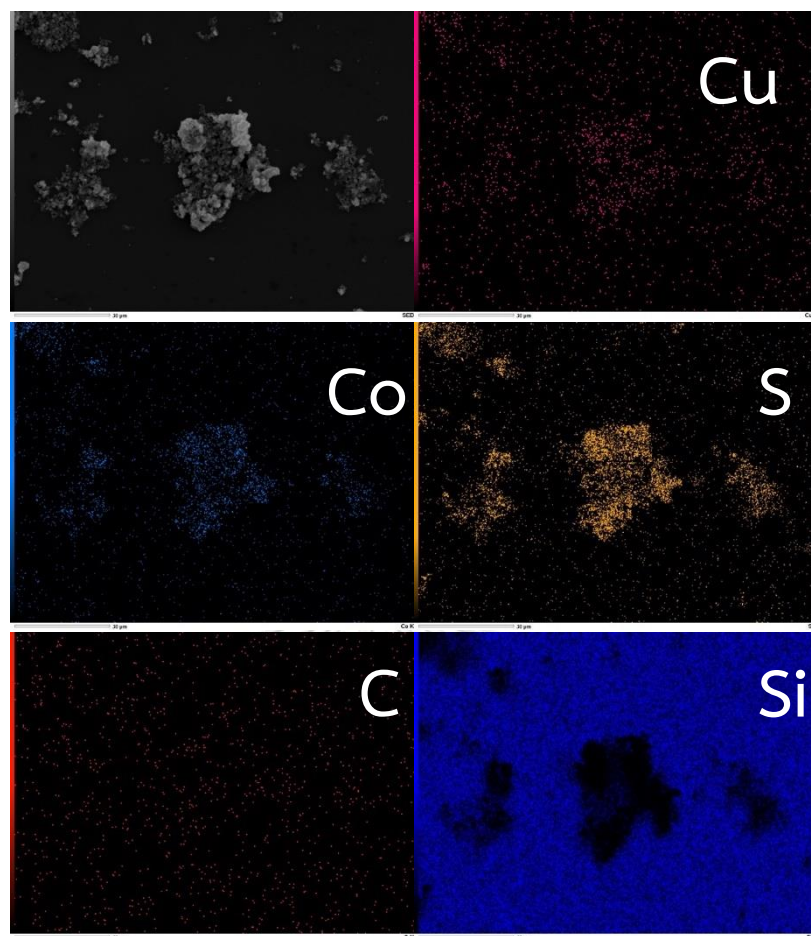


Figure 15 EDS elemental mapping images of CuCo_2S_4

Table 7 Elemental percentages of CuCo_2S_4

Formula	mass%	Atom%	Sigma	Net	K ratio	Line
C	9.19	19.57	0.07	2169	0.000693	K
Si	83.7	76.21	0.13	1502340	0.585549	K
S	3.22	2.57	0.03	26182	0.012314	K
Co	2.65	1.15	0.04	10254	0.016797	K
Cu	1.24	0.5	0.05	3454	0.007841	K
Total	100	100				

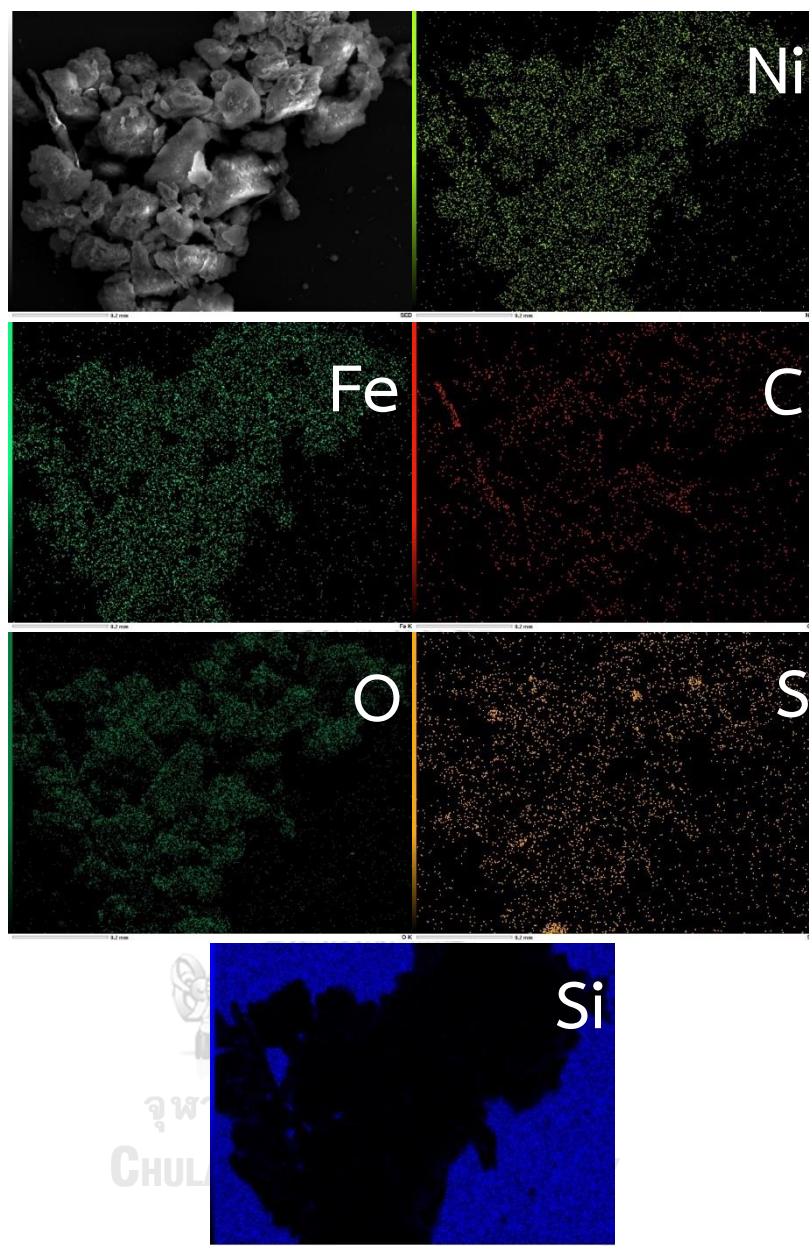


Figure 16 EDS elemental mapping images of $18\text{CuCo}_2\text{S}_4/\text{NiFe}$ LDH

Table 8 Elemental percentages of $18\text{CuCo}_2\text{S}_4/\text{NiFe}$ LDH

Formula	mass%	Atom%	Sigma	Net	K ratio	Line
C	9.48	19.62	0.04	4408	0.001397	K
O	17.89	27.79	0.07	47427	0.051048	K
Si	46.16	40.85	0.11	627704	0.24273	K
S	0.87	0.67	0.02	8393	0.003917	K
Fe	10.42	4.64	0.06	49901	0.068789	K
Ni	15.18	6.43	0.09	52635	0.102038	K
Total	100	100				



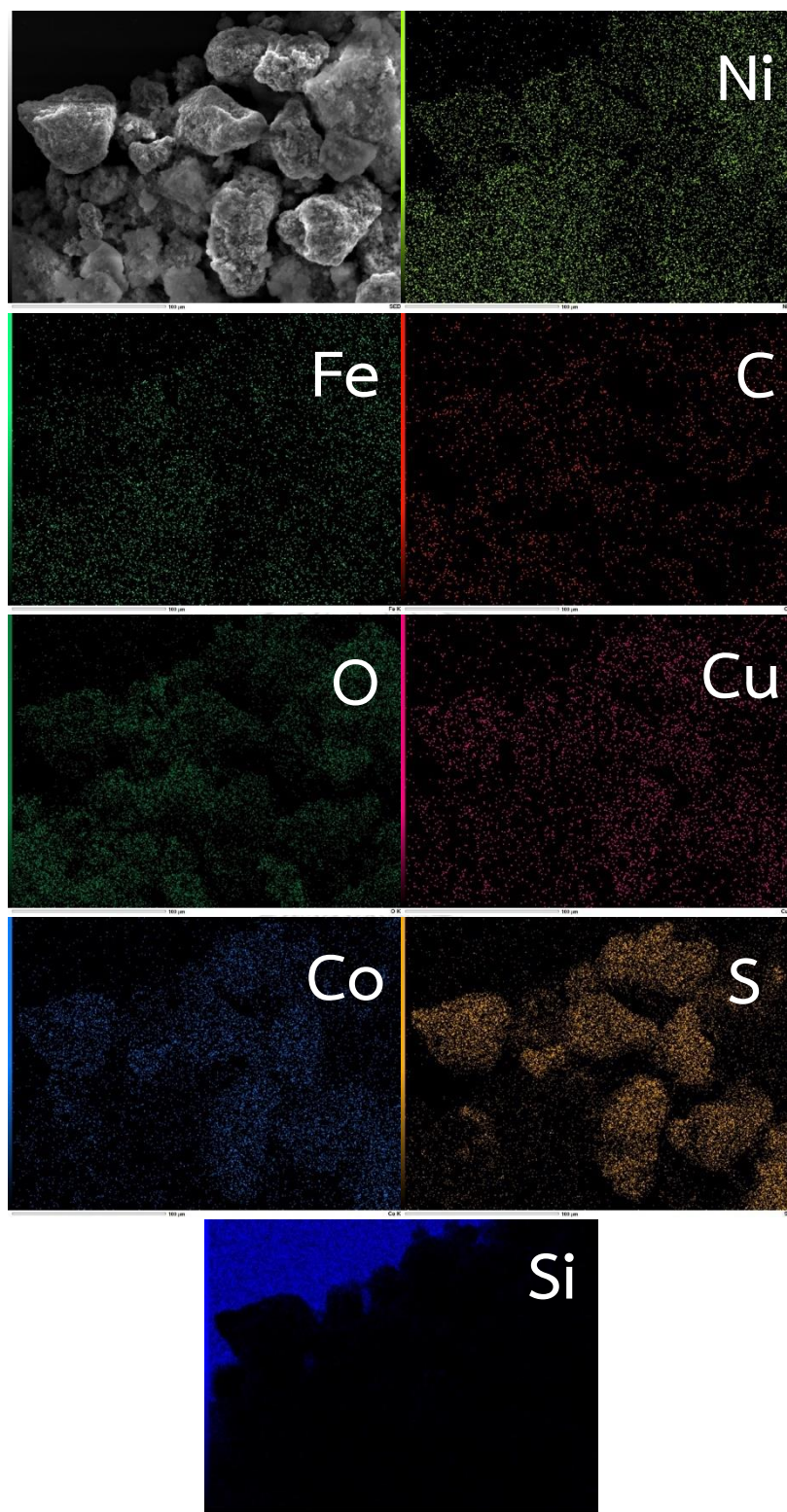


Figure 17 EDS elemental mapping images of $34\text{CuCo}_2\text{S}_4/\text{NiFe}$ LDH

Table 9 Elemental percentages of $^{34}\text{CuCo}_2\text{S}_4/\text{NiFe}$ LDH

Formula	mass%	Atom%	Sigma	Net	K ratio	Line
C	7.55	17.47	0.04	4510	0.001427	K
O	18.62	32.36	0.06	56682	0.060908	K
Si	23	22.76	0.08	268323	0.103585	K
S	8.55	7.41	0.04	92383	0.043038	K
Fe	6.19	3.08	0.05	30404	0.041842	K
Co	10.17	4.8	0.07	41247	0.066921	K
Ni	21.7	10.27	0.11	76442	0.147944	K
Cu	4.21	1.84	0.07	12091	0.027186	K
Total	100	100				

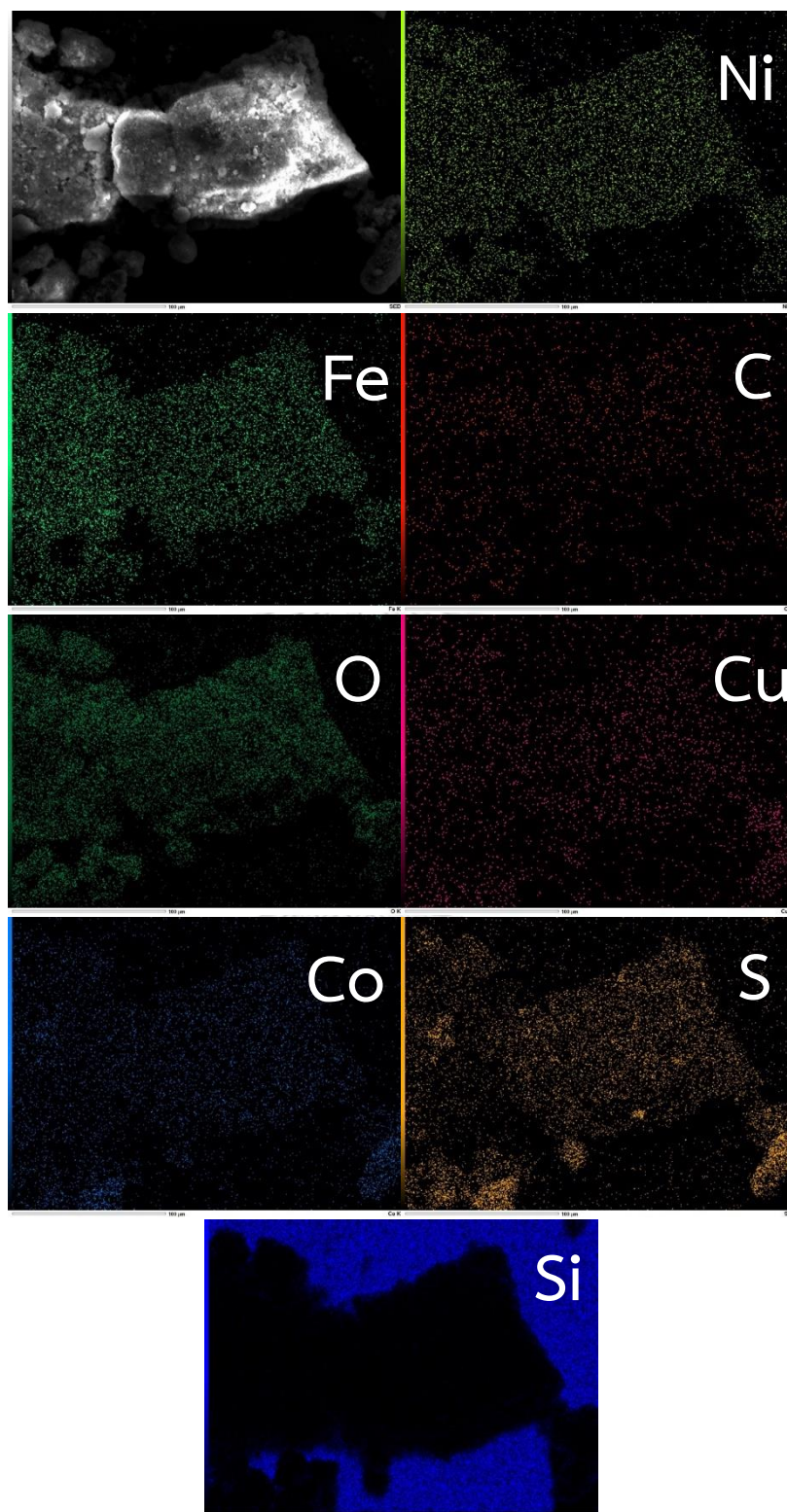
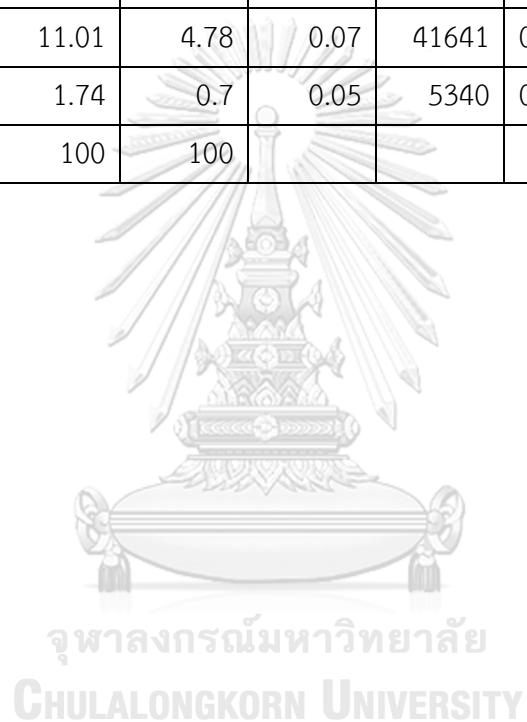


Figure 18 EDS elemental images of $52\text{CuCo}_2\text{S}_4/\text{NiFe LDH}$

Table 10 Elemental percentages of $52\text{CuCo}_2\text{S}_4/\text{NiFe LDH}$

Formula	mass%	Atom%	Sigma	Net	K ratio	Line
C	6.96	14.78	0.04	3544	0.001124	K
O	20.31	32.35	0.07	62551	0.067389	K
Si	42.01	38.12	0.1	609645	0.235959	K
S	3.46	2.75	0.03	37282	0.017413	K
Fe	10.65	4.86	0.06	55660	0.076796	K
Co	3.84	1.66	0.05	16708	0.027178	K
Ni	11.01	4.78	0.07	41641	0.080799	K
Cu	1.74	0.7	0.05	5340	0.012038	K
Total	100	100				



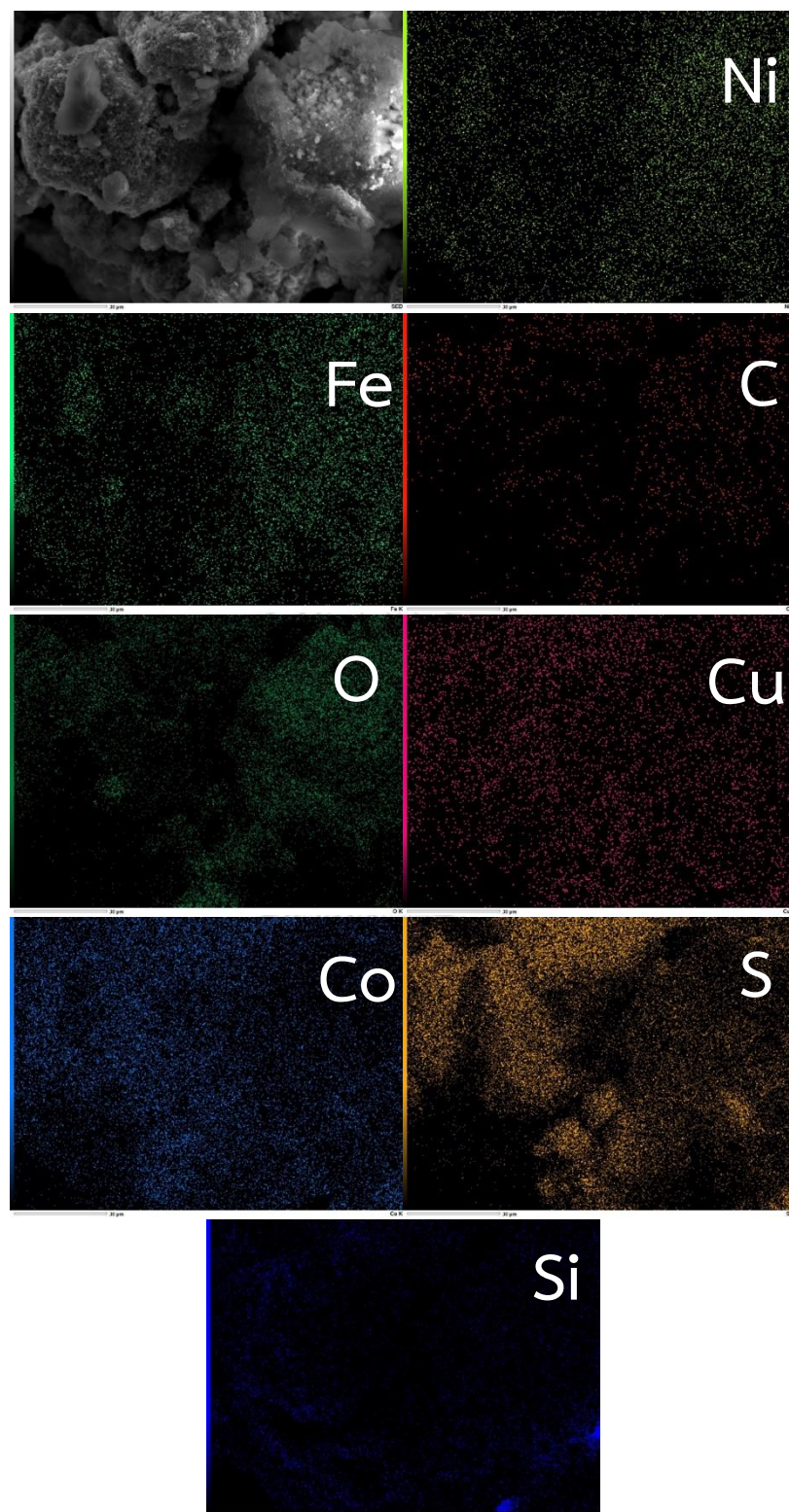


Figure 19 EDS elemental images of $99\text{CuCo}_2\text{S}_4/\text{NiFe LDH}$

Table 11 Elemental percentages of 99CuCo₂S₄/NiFe LDH

Formula	mass%	Atom%	Sigma	Net	K ratio	Line
C	5.06	13.48	0.03	3016	0.000951	K
O	18.31	36.63	0.07	51067	0.054706	K
Si	2.29	2.61	0.04	18684	0.007191	K
S	15.26	15.23	0.05	143345	0.066574	K
Fe	10.5	6.02	0.07	41070	0.056346	K
Co	24.55	13.33	0.11	78896	0.127611	K
Ni	14.65	7.98	0.11	40834	0.078786	K
Cu	9.37	4.72	0.11	21171	0.047455	K
Total	100	100				

4.3 Inductively coupled plasma optical emission spectroscopy (ICP-OES)

The molar ratios of Ni to Fe and Cu to Co in materials were investigated by ICP-OES and EDS elemental mapping in Table 12-13. The result in Table 8 showed the maintenance of the molar ratios of Cu to Co in catalyst indicating preparation of composite using hydrothermal method have not be effected to CuCo₂S₄

Table 12 The molar ratios of Ni:Fe of initials and final value

Sample name	The molar ratio of Ni:Fe	
	Initial value	Final value (ICP)
NiFe LDH	3 : 1	1.25 : 1
18CuCo ₂ S ₄ /NiFe LDH	3 : 1	1.58 : 1
34CuCo ₂ S ₄ /NiFe LDH	3 : 1	2.55 : 1
52CuCo ₂ S ₄ /NiFe LDH	3 : 1	0.91 : 1
99CuCo ₂ S ₄ /NiFe LDH	3 : 1	0.88 : 1

Table 13 The molar ratios of Cu:Co of initials value and final value

Sample name	The molar ratio of Cu:Co	
	Initial value	Final value (ICP)
CuCo ₂ S ₄	1 : 2	1 : 1.77
18CuCo ₂ S ₄ /NiFe LDH	1 : 2	1 : 2.00
34CuCo ₂ S ₄ /NiFe LDH	1 : 2	1 : 1.89
52CuCo ₂ S ₄ /NiFe LDH	1 : 2	1 : 1.98
99CuCo ₂ S ₄ /NiFe LDH	1 : 2	1 : 1.91

4.4 Catalytic performance

Degradation of methylene blue was evaluated as shown in Fig. 20. Methylene blue self-degradation was almost negligible which can be seen from the blank experiment. Pure NiFe LDH showed a slow dye degradation to 19.4%. Loading of CuCo₂S₄ displayed superior degradation percentage to pure NiFe LDH. 18CuCo₂S₄/NiFe LDH was found to be the highest catalytic performance with 97.9% of methylene blue degradation. Over loading of CuCo₂S₄ contributed to reduce of catalytic activity. However, activity of all of composites was higher than pure CuCo₂S₄ based on the same Cu content.

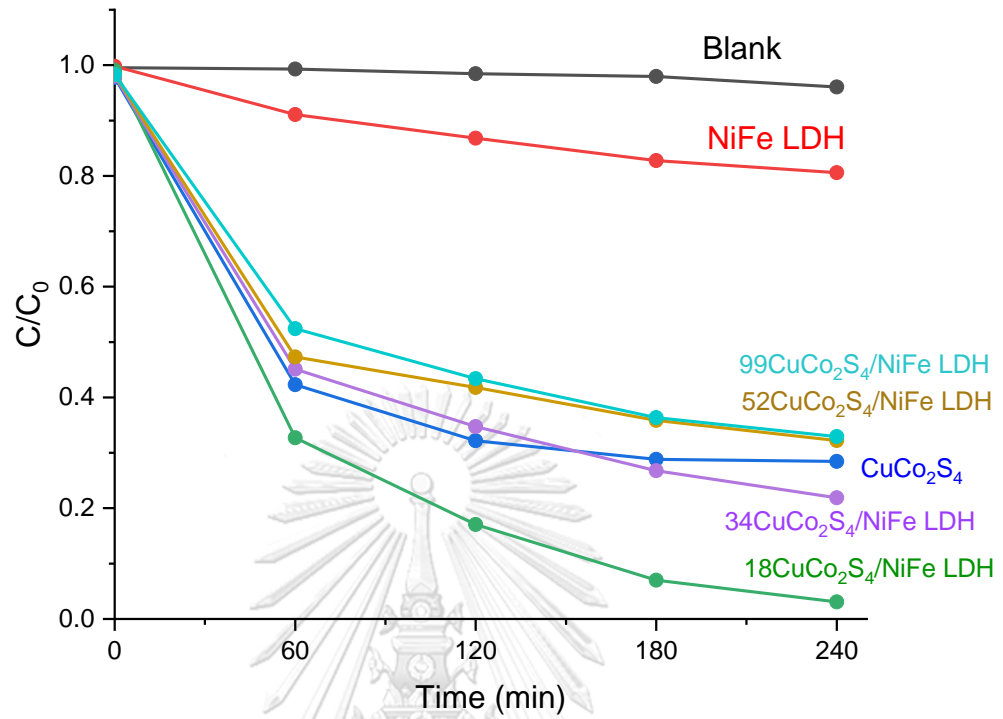


Figure 20 Degradation of methylene blue on CuCo₂S₄/NiFe LDH

4.4.1 Effect of H₂O₂

To identify the optimal reaction conditions for the methylene blue degradation, 18CuCo₂S₄/NiFe LDH was used as a catalyst.

Effect of H₂O₂ volume on dye degradation was investigated. Fig. 21 showed that addition of 100 μ L of H₂O₂ provided 65% dye degradation, while the addition in the range of 200-600 μ L of H₂O₂ reached almost 98% in 4h. Excess of H₂O₂ may cause decomposition of CuCo₂S₄. Therefore, 200 μ L of H₂O₂ was set as an optimized condition.

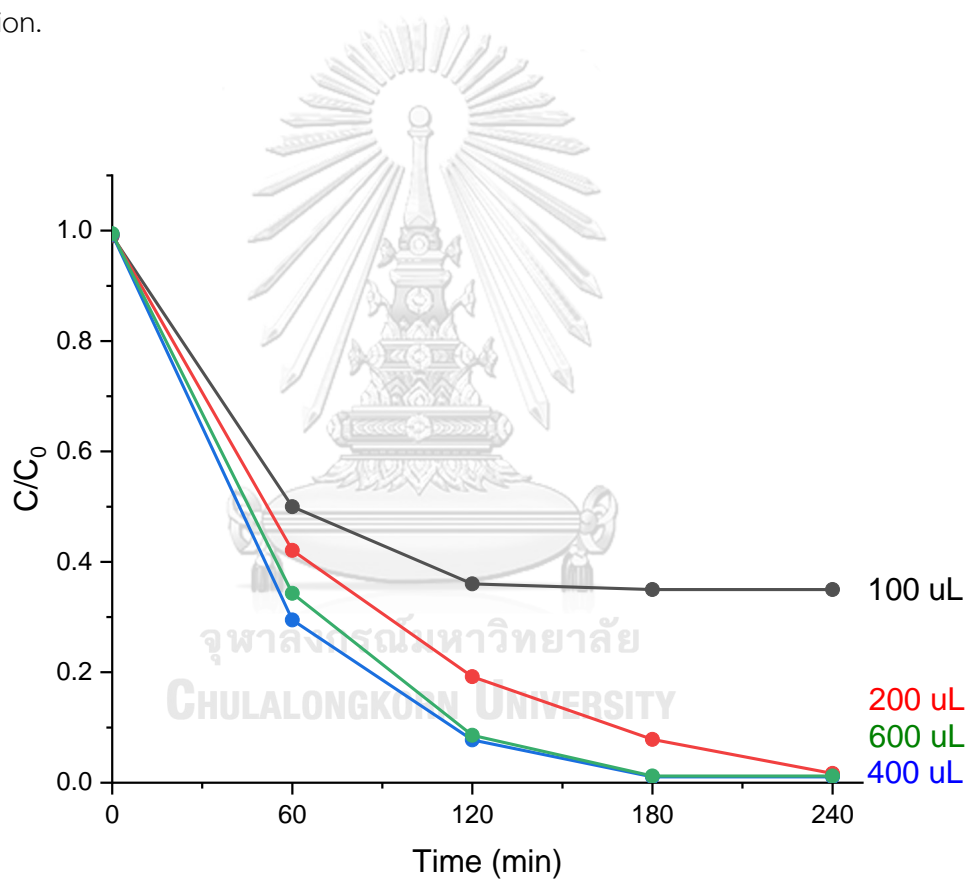


Figure 21 Effect of H₂O₂ volume on dye degradation

4.4.2 Effect of catalyst dosage

Effect of catalyst dosage in Fig. 22 showed that 5 mg of catalyst performed 85% of dye degradation. 10 mg of catalyst caused higher dye removal efficiency due to the increasing of active site of catalyst. When the catalyst dosage was increased higher than 10 mg, no significantly changes occurred according to saturation of catalyst dosage.

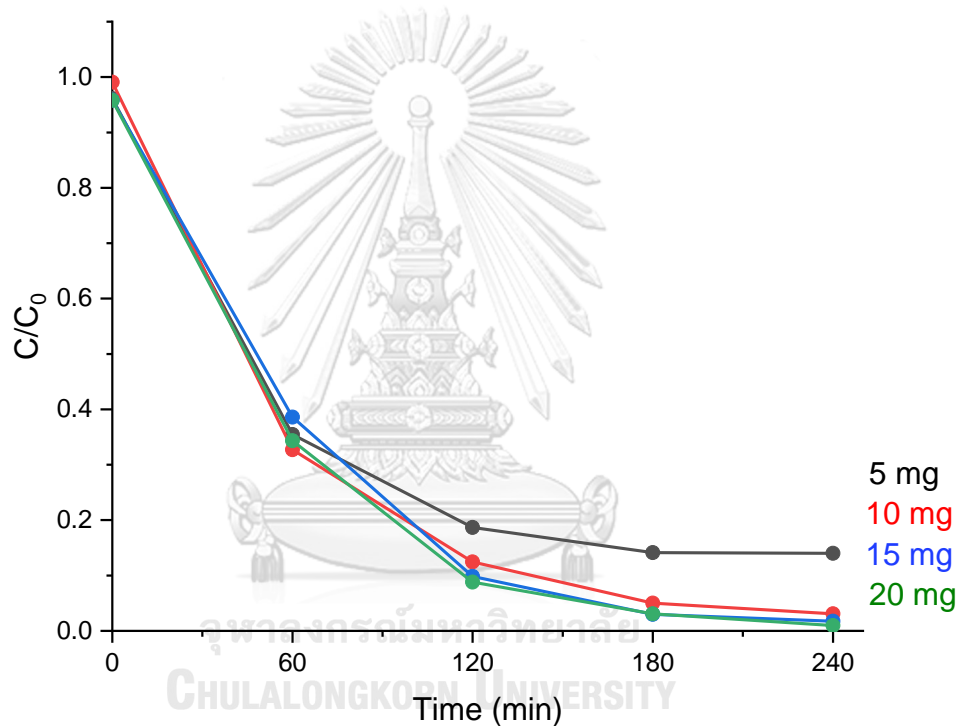


Figure 22 Effect of catalyst dosage on dye degradation

4.4.3 Effect of dye concentration

Effect of dye concentration in Fig. 23 indicated that methylene blue degradation decreased with the increase of the dye from 5-20 ppm

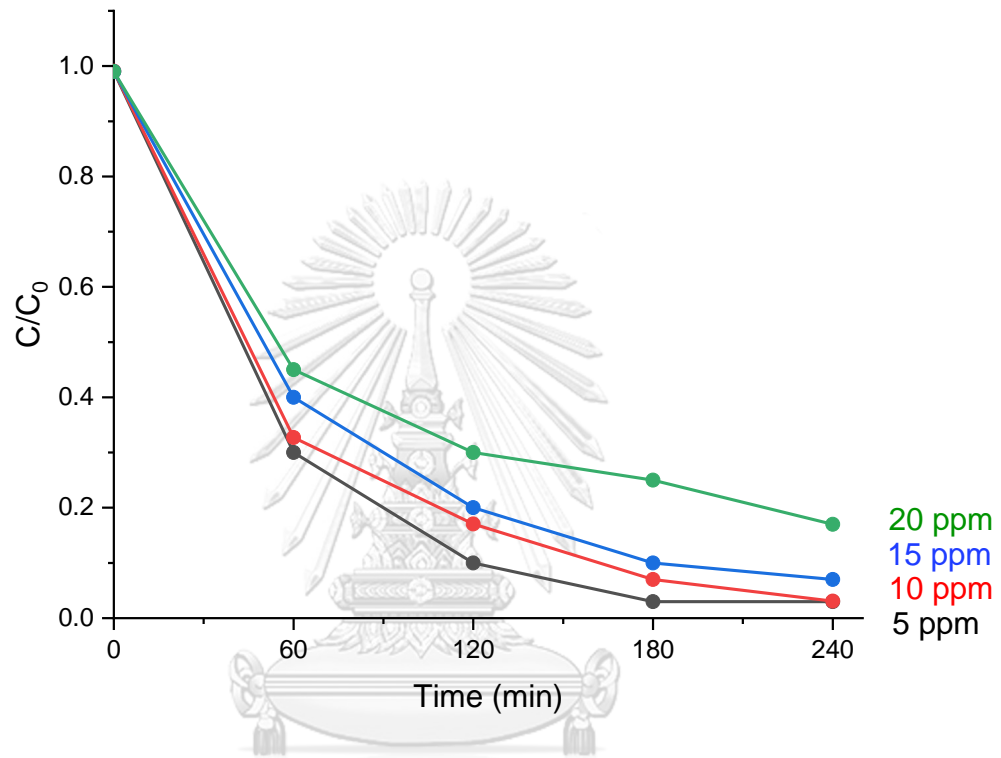


Figure 23 Effect of methylene blue concentration on dye degradation

4.4.4 Effect of pH

Effect of pH is considered as the main parameter in catalytic process. Fig. 24 clearly showed the highest performance at pH 3, which means that catalyst performed mainly through the active sites. Under acidic condition, concentration of H^+ ion in the reaction system increased leading to enhancing of reaction between active site on the surface of $CuCo_2S_4$ and H^+ to produce active species for degradation resulting in low concentration of methylene blue^{11,12}. However, at acidic system provided solubility of metal ions during the reaction time of 4 h as shown in Table 14. pH 3 may not be the best condition due to the highest metal leaching, which could affect to the environment. Therefore, neutral pH could be used as the optimal condition.

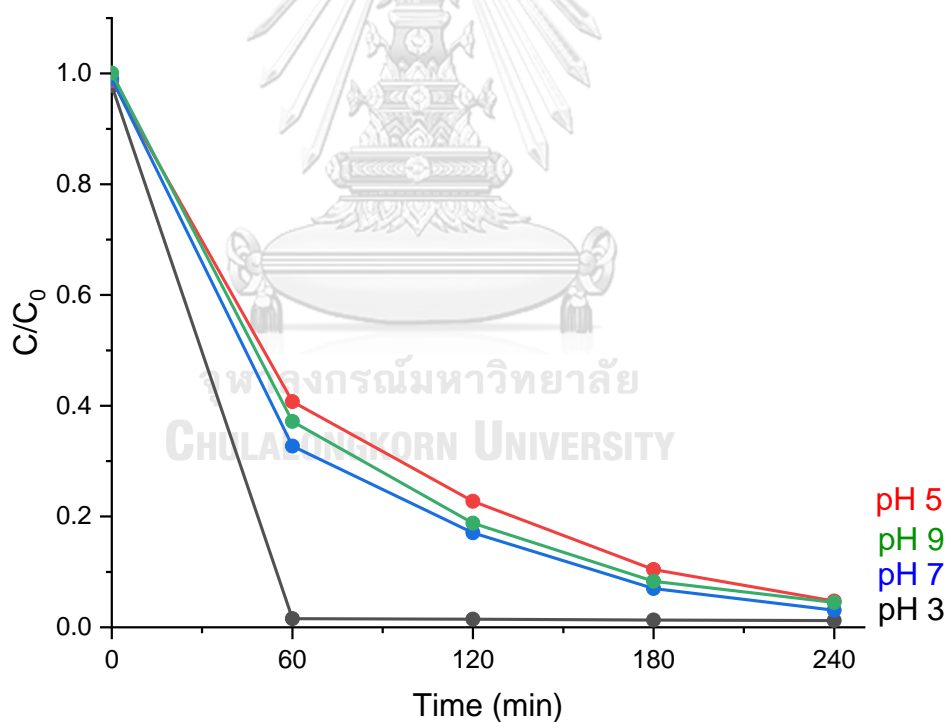
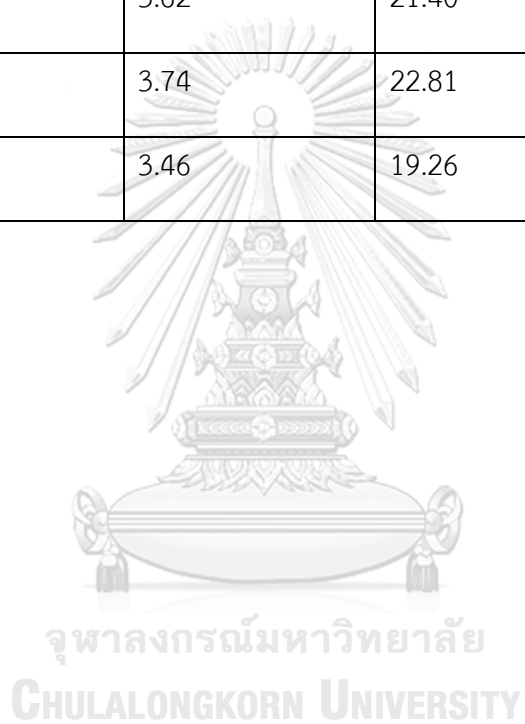


Figure 24 Effect of pH on dye degradation

Table 14 Metal leaching in the reaction mixture at different pH after Fenton reaction

pH	Cu (ppm)	Co (ppm)	Ni (ppm)	Fe (ppm)
3	12.22	8.38	117.30	nd
5	0.73	3.62	21.40	nd
7	0.46	3.74	22.81	nd
9	0.48	3.46	19.26	nd

nd= not detected



4.5 Catalytic mechanism

In order to propose the catalytic mechanism, the different scavengers were added to the system to capture reactive species such as IPA, DMSO, and p-BQ for scavenging $\bullet\text{OH}$, e^- and $\bullet\text{O}_2^-$, respectively. Addition of 5 mmol of IPA, DMSO, and p-BQ as shown in Fig 25, showed the decrease of methylene blue degradation from 98 to 16, 11 and 94, respectively. As a result, $\bullet\text{OH}$, e^- and $\bullet\text{O}_2^-$ were formed in the Fenton solution reaction.

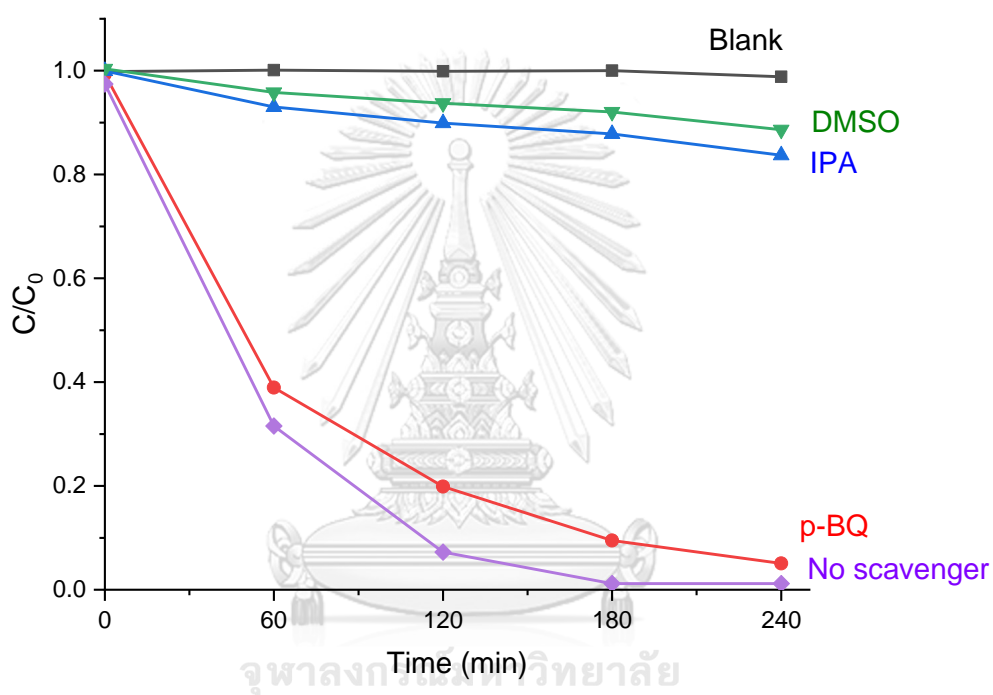
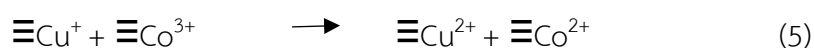
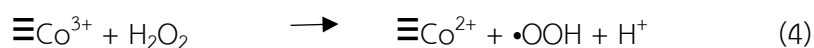
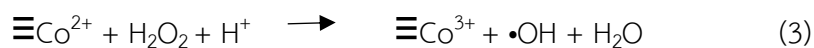
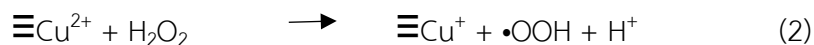
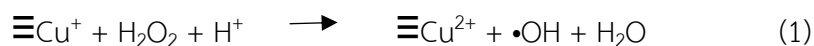


Figure 25 Effect of various scavengers on dye degradation

On the basis of effect of pH and different trapping agents, the mechanism related to Fenton reaction were demonstrated following equations [19]



$\equiv\text{Cu}^+$ was oxidized by H_2O_2 to produce $\equiv\text{Cu}^{2+}$ and H_2O_2 was activate to $\cdot\text{OH}$ as equation (1). $\equiv\text{Cu}^{2+}$ activated H_2O_2 to $\cdot\text{OOH}$ and $\equiv\text{Cu}^+$ was formed by reduction reaction of $\equiv\text{Cu}^{2+}$ as equation (2). $\equiv\text{Co}^{2+}$ was reacted similarly to $\equiv\text{Cu}^+$ as equation (3) and (4). In acidic condition, H^+ in the system enhanced production of $\cdot\text{OH}$ and $\cdot\text{OOH}$ as equation (1), (3) and (6). $\cdot\text{OH}$ and $\cdot\text{O}_2^-$ oxidized MB to degradation product as equation (7) and (8).

Moreover, electron from CuCo_2S_4 can move to NiFe LDH due to the excellent electron conductivity of NiFe LDH, which promotes the redox rate of the Fenton-like reaction cycle leading to the increase in the degradation of the dye. The scheme with mechanism as shown in Fig. 26.

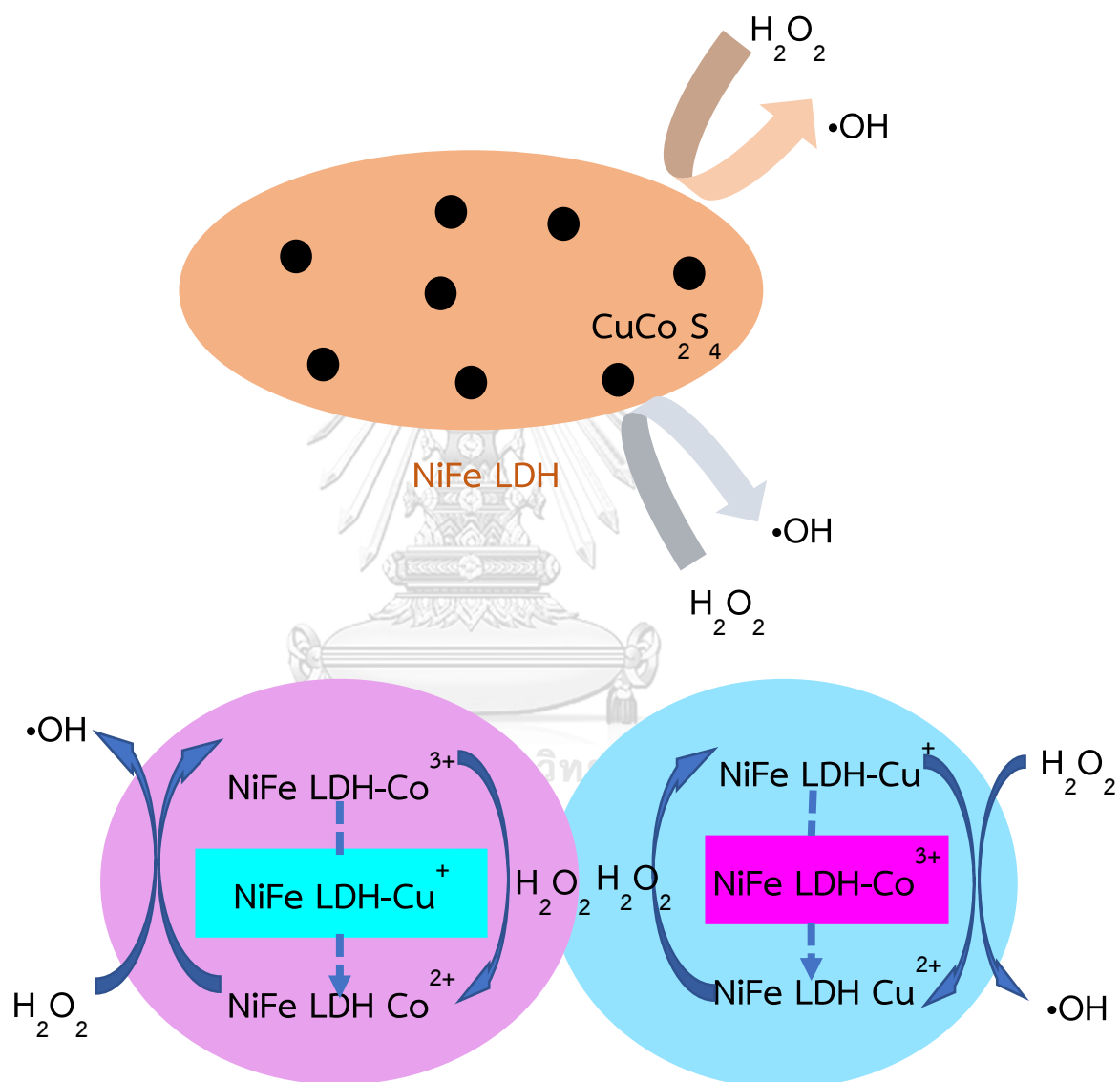


Figure 26 Scheme illustrating the mechanism of the enhance catalytic process of $\text{CuCo}_2\text{S}_4/\text{NiFeLDH}$

CHAPTER V CONCLUSION

5.1 Conclusion

CuCo₂S₄/NiFe LDH composites with varied content of CuCo₂S₄ from 1.8 wt% to 9.9 wt% over NiFe LDH were successfully synthesized using hydrothermal process. XRD suggested co-existence of CuCo₂S₄ and NiFe LDH for the composite catalysts. SEM images showed uniformly distribution of elementals. 18CuCo₂S₄/NiFe LDH was found to be the best catalyst for methylene blue degradation through Fenton reaction. The highest efficiency of 98% was achieved at pH value of 7 with low metal leaching during 240 min of reaction time. The mechanisms were studied by addition of various scavengers to trap active radicals. •OH, electron and •O₂⁻ were found in the solution system confirming decomposition of H₂O₂ through Fenton-like processes.

5.2 Recommendations for future work

1. Various of dyes should be studied.
2. Determination of catalytic active site should be reported.

REFERENCES

1. Xing, M., et al., *Metal Sulfides as Excellent Co-catalysts for H₂O₂ Decomposition in Advanced Oxidation Processes*. Chem, 2018. **4**(6): p. 1359-1372.
2. Phan, T.T.N., et al., *Adsorption and photo-Fenton catalytic degradation of organic dyes over crystalline LaFeO₃-doped porous silica*. RSC Adv, 2018. **8**(63): p. 36181-36190.
3. Wang, Y., et al., *2D material based heterostructures for solar light driven photocatalytic H₂ production*. Materials Advances, 2022. **3**(8): p. 3389-3417.
4. Gonçalves, R.G.L., et al., *Fenton-like degradation of methylene blue using Mg/Fe and MnMg/Fe layered double hydroxides as reusable catalysts*. Applied Clay Science, 2020. **187**.
5. Nayak, S., G. Swain, and K. Parida, *Enhanced Photocatalytic Activities of RhB Degradation and H₂ Evolution from in Situ Formation of the Electrostatic Heterostructure MoS₂/NiFe LDH Nanocomposite through the Z-Scheme Mechanism via p-n Heterojunctions*. ACS Appl Mater Interfaces, 2019. **11**(23): p. 20923-20942.
6. Zhang, M., et al., *Multiwalled carbon nanotube-supported CuCo₂S₄ as a heterogeneous Fenton-like catalyst with enhanced performance*. RSC Advances, 2017. **7**(34): p. 20724-20731.
7. Wu, M.J., et al., *A review on fabricating heterostructures from layered double hydroxides for enhanced photocatalytic activities*. Catalysis Science & Technology, 2018. **8**(5): p. 1207-1228.
8. Zhang, J., et al., *Photocatalytic and degradation mechanisms of anatase TiO₂: a HRTEM study*. Catalysis Science & Technology, 2011. **1**(2).
9. Mahmoud, M.S., J.Y. Farah, and T.E. Farrag, *Enhanced removal of Methylene Blue by electrocoagulation using iron electrodes*. Egyptian Journal of Petroleum, 2013. **22**(1): p. 211-216.

10. Khan, I., et al., *Review on Methylene Blue: Its Properties, Uses, Toxicity and Photodegradation*. *Water*, 2022. **14**(2).
11. Kurian, M., *Advanced oxidation processes and nanomaterials -a review*. *Cleaner Engineering and Technology*, 2021. **2**.
12. Weiss, J. *Reaction Mechanism of Oxidation-Reduction Processes*. *Nature*, 1934: p 648-649.
13. Li, T., H. Miras, and Y.-F. Song, *Polyoxometalate (POM)-Layered Double Hydroxides (LDH) Composite Materials: Design and Catalytic Applications*. *Catalysts*, 2017. **7**(9).
14. Aragaw, S.G., et al., *Synthesis of CuAl-layered double hydroxide/MgO₂ nanocomposite catalyst for the degradation of organic dye under dark condition*. *Applied Water Science*, 2022. **12**(6).
15. Wang, Q., X. Wang, and B. Tian, *Catalytic performances of Ni/Fe layered double hydroxides fabricated via different methods in Fenton-like processes*. *Water Sci Technol*, 2018. **77**(11-12): p. 2772-2780.
16. Li, Z., et al., *Three-dimensional CuS hierarchical architectures as recyclable catalysts for dye decolorization*. *CrystEngComm*, 2012. **14**(11).
17. Chauhan, M., et al., *Promising visible-light driven hydrogen production from water on a highly efficient CuCo₂S₄ nanosheet photocatalyst*. *Journal of Materials Chemistry A*, 2019. **7**(12): p. 6985-6994.
18. Wu, X., et al., *Fabrication of NiFe layered double hydroxides using urea hydrolysis—Control of interlayer anion and investigation on their catalytic performance*. *Catalysis Communications*, 2014. **50**: p. 44-48.
19. He, M. and Z. Nan, *3D-structured CuCo₂S₄ as an excellent Fenton-like catalyst under alkaline solution*. *Powder Technology*, 2020. **376**: p. 263-271.



จุฬาลงกรณ์มหาวิทยาลัย
CHULALONGKORN UNIVERSITY

VITA

NAME Ajjirawadee Suwanchan
DATE OF BIRTH 20 November 1994
PLACE OF BIRTH Songkhla
HOME ADDRESS 226/4 Sriyuthaya road Dusit Bangkok 10300



จุฬาลงกรณ์มหาวิทยาลัย
CHULALONGKORN UNIVERSITY